RESEARCH PAPER

Sodium Alginate Nanoparticle Dry Powder Inhaler for Pulmonary Co-Delivery of WHO-Recommended Anti-Tuberculosis Medications

Pooja Singh [1], Bhavna Kumar[2] , Dr. Santosh Kumar Verma [3]
[1]DIT UNIVERSITY, DEHARADUN [2]DIT UNIVERSITY, DEHERADUN
[3]QUANTUM UNIVERSITY, ROORKEE

ABSTRACT
Tuberculosis (TB) is a major cause of preventable deaths and a chronic worldwide health concern. Pulmonary delivery of drugs via inhalable routes has been recommended over systemic administration (such as intravenous or oral) in order to achieve localized distribution of drugs to the lung with enhanced therapeutics and lowered systemic adverse effects. The combination of multiple drugs loaded nanoparticles in a single dosage form like DPI offers a unique therapeutic advantage for simultaneously delivering drug payloads to the intracellular infection sites in predefined ratios. The study aimed to co-administer four WHO-recommended anti-TB drugs, isoniazid, rifampicin, pyrazinamide, and moxifloxacin Hcl, using a sodium alginate polymeric nanoparticle DPI to facilitate their pulmonary administration for effective treatment of TB-infected individuals. The ATDs (isoniazid, rifampicin, pyrazinamide, and moxifloxacin Hcl) loaded sodium alginate nanoparticle separately was prepared using the Emulsification/internal gelation technique. The percentage drug entrapment, drug loading and particle size were of isoniazid nanoparticles, rifampicin nanoparticles, Pyrazinamide nanoparticles and moxifloxacin Hcl nanoparticles were observed to be 76.632±0.448%, 75.260±0.101%, 76.797±0.293%, 77.252±0.086%; 21.261±0.254%, 32.036±0.352%, 14.196±0.458%, 16.480±0.017%; 199.167 ±0.777nm, 221.77 ±1.645nm, 273.157 ±4.117nm and 250.327 ±0.818nm. The PDI of the all four nanoparticles' formulations was observed to be less than 0.2, while high zeta potential value indicated the stability of the formulation. The FTIR, XRD and DSC study confirmed the encapsulation of drug in the nanoparticles. TEM Images confirmed the spherical shape of drug loaded nanoparticles. In the next step, all four ATDs nanoparticles were combined, mixed with the carriers (lactose, leucin, and mannitol), and transformed in the DPI formulation. The lactose containing nanoparticles DPI formulation yielded the better flow property. In vitro drug release study demonstrated that the ATDs combined nanoparticle DPI formulation yielded the sustained release profile of the drug than the blend of the API. In vivo pharmacokinetic study demonstrated the mean residence time (MRT) of a combination of ATDs loaded DPI formulation was between 34-46 hours. Furthermore, an increase in AUC value in the lung for the combination of ATDs loaded DPI formulation compared with the AUC of blend of ATDs DPI. The increase in AUC of the ATDs combined nanoparticle DPI formulation could be attributed, at least in part, to the prolonged retention and reduced alveolar clearance of drug-loaded nanoparticles from lung tissue compared to blend of ATDs drug DPI..

Keywords: ATDs: Antituberculosis drug, DPI: Dry powder inhaler, TB: Tuberculosis, AM: Alveolar microphases, INH: Isoniazid, PZA: Pyrazinamide, RIF: Rifampicin and MHCl: Moxifloxacin hydrochloride.
How to cite this article: Singh P, Kumar B, Verma SK, Sodium Alginate Nanoparticle Dry Powder Inhaler for Pulmonary Co-Delivery of WHO-Recommended Anti-Tuberculosis Medications. .Int J Drug Deliv Technol. 2026;16(2s): 587-609; DOI: 10.25258/ijddt.16. 587-609
Source of support:. None
Conflict of interest: None

INTRODUCTION

Tuberculosis (TB), a worldwide disease accountable for death and morbidity. As per report approximate in every year 10.0 Lac patients die due to tuberculosis, and an estimated 10 million more get the disease (1). India endures almost 25% of the world's TB burden, with a no. of TB cases 2.77 million in 2022 (2). Tuberculosis (TB) (3), a chronic worldwide health concern, and a significant socioeconomic burden on developing and underdeveloped nations (4). Mycobacterium tuberculosis is an intracellular organism that causes TB infection when it is inhaled (5).

In the human body, tuberculosis spreads through a vector called the mycobacterium tuberculosis. It invades the human body through the phagocytosis process, which is caused by the interaction between the alveolar macrophages' (AM) surface mannose receptors and lipoarabinomannan (4). The pathogenesis of tuberculosis is triggered by the inhalation and interaction of the bacilli spread in the air through 'alveolar' 'macrophages. Following this, nearby alveolar macrophages proliferate and invade the area. The most well-established target for TB treatment is alveolar macrophages, even though dendritic cells and epithelial type II pneumocytes also play a role in the prognosis of TB (6).

Tuberculosis growing day by day at faster rate due to the long treatment period (6 months) of conventional drugs and the dearth of patient-adherent therapeutic choices. Additionally, multidrug-resistant strains and mycobacteria in low proliferative stages require longer treatment periods

**Author for Correspondence: bhavnano@gmail.com*

of more than 24 months (4). TB-DOTS (directly observed therapy, short-course) is the treatment regimen used to treat TB patients. Rifampicin (RIF), Isoniazid, Ethambutol, moxifloxacin, and Pyrazinamide, either alone or in combination, are among the chemotherapy drugs utilized for the treatment (3).

Severa reasons like low aqueous solubility of active ingredient, less availability of active to the infection site, degradation of active in GIT tract, higher side effect, and higher duration for time period, all of which contribute to non-compliance, the current conventional oral therapy is ineffective and frequently fails to fully cure patients. Furthermore, the multi-drug regimen is particularly susceptible to adverse effects such as hepatotoxicity, skin rashes, nausea, vomiting, and epigastric pain. One of the main issues is noncompliance with prescribed regimens because treating tuberculosis requires regular, ongoing multiple drug administration (3).

Furthermore, several problems, such as a protracted treatment protocol, the need for extremely high doses, and severe toxicity, contribute to poor patient compliance with the therapy regimen (7).

Treating respiratory infections has traditionally been extremely challenging since the bacteria that cause respiratory infections locate deep within the lungs, and less amount of active ingredient can reach the lungs following oral or parenteral delivery. Thus, a higher dose of the drug regimen is required to keep the amount of active above the minimal inhibitory concentration (8).

Pulmonary administration of active ingredient via inhalable routes has been recommended over systemic administration in order to achieve localized distribution of drugs to the lung with enhanced therapeutics and lowered systemic adverse effects (9). Comparing the pulmonary route of administration to traditional oral medication, there are several benefits, including increased drug “bioavailability”, improved “patient”, decreased systemic side effects, and longer drug action (10-12).

Inhaled drug delivery allows the drug to directly reach to the site of action, shortens the treatment period, ensures a rapid onset of action, and hinders drug “resistance” and significant adverse effects (13-16). The conventional drug delivery methods are unable to deliver the antitubercular drug to the alveolar region because they are delivered indirectly through the blood, Therefore, novel strategies must be developed for efficient pulmonary drug administration that prevents off-target accumulation. Since the causative agent is found in the host AM, a targeted delivery may be achieved by designing an inhalation device with a favorable aerodynamic profile, perhaps lowering the frequency of dosages (17).

Recent developments in nanotechnology have generated a lot of interest in using nanoparticles as drug delivery vehicles in the lungs. Inhalable nanoparticle-based drug delivery systems have several distinct advantages over traditional inhalable formulations, which contain the drug either in suspension or solution form (e.g., as formulations for use in nebulizers) or as micronized dry particles in conventional inhalable dry powder formulations (18).

First, nanoparticles can be surface-modified by ligands (such as peptides, antibodies, etc.) to target particular lung cell types, such as lung tumor cells (19). Second, Nanoparticles smaller than 300 nm can evade macrophage absorption and shield the drug payload from enzymatic destruction (20). Thirdly, nanoparticles can enhance delivery of drug into cells more effectively than free drugs by using different endocytosis-based mechanisms (21). Fourthly, altering the characteristics of the nanocarrier can allow for the controlled or even prolonged release of drugs (22).

Most importantly, nanoparticles can easily deliver from alveoli to the systemic circulation, but microparticles are unable to do so. This implies that there is an alternate way to administer nanoparticles throughout the body without requiring intrusive intravenous administration (23). This characteristic is especially helpful for diseases that have both systemic and lung symptoms (e.g., tuberculosis, metastasized lung malignancies, etc.). Inhalable nano systems with various compositions have also been extensively and effectively studied in the past. Of these, polymeric nanosystems are beneficial because to their potential to translocate across biological barriers, controlled release profile, desired pharmacokinetic consequences, and the ability to encapsulate both hydrophilic and hydrophobic medicines (17).

DPI devices are more streamlined and user-friendly than other inhaler devices and have the ability to administer many drugs at once in the same aerosol similar to the FDA approved dual-drug and triple-drug DPIs (24). FDA approved the DPIs to be used in youngsters as young as four years old. For DPIs, the solid state offers advantages in terms of physical and chemical stability, and propellants are not used.

The combination of multiple drugs loaded nanoparticles in a single dosage form like DPI offers a unique therapeutic advantage for simultaneously delivering drug payloads to the intracellular infection sites in predefined ratios (25).

The study aimed to co-administer four WHO-recommended anti-TB drugs isoniazid, rifampicin, rifampicin, and moxifloxacin Hcl using a polysaccharide polymeric nanoparticle DPI to facilitate their pulmonary administration for effective treatment of TB-infected individuals. Sodium alginate, a natural polymer with characteristics like an aqueous matrix environment, high gel porosity, and biocompatibility, was utilized to prepare antituberculosis drug loaded nanoparticles. The US Food and Drug Administration (FDA) has approved sodium alginate for oral use (26). Sodium alginate nanoparticles containing isoniazid (INH), pyrazinamide (PZA), rifampicin (RIF), and moxifloxacin Hcl (MHcl) were prepared separately and co-administered in the DPI formulation. The prepared ATDs loaded solidum alginate nanoparticles co-administered with DPI were characterized for in vitro parameters and pharmacokinetic parameters through the pulmonary route.

1.1 Material

Isoniazid and Rifampicin were procured from the SRL. The pyrazinamide was procured from the TCI. The

moxifloxacin was procured from GLR.Sodium alginate was procured from the Thomas baker. The light liquid paraffin was procured from the Qualikems.

1.2 Experimental work

1.2.1 Preparation of ATDs loaded solidum alginate nanoparticles

The ATDs loaded sodium alginate nano size range particles was prepared using the Emulsification/internal gelation technique. The accurately measured amount of the ATDs was transferred to a beaker containing water and sonicated for 5 minutes, resulting in a clear solution. The accurately weighed amount of sodium alginate was transferred to a beaker containing the drug's aqueous solution with the aid of heat at 100 rpm using a magnetic stirrer. In the meantime, the measured amount of Span 80 was blended with the light liquid paraffin by homogenizing at 5000 rpm for 20s. The aqueous drug containing polymeric solution was emulsified in the liquid paraffin solution by homogenizing at 5000 rpm for 30s. After the emulsification, the calcium chloride aqueous solution was dispersed to the emulsion, and homogenization was continued again for 20s followed by probe sonicated. Pure isopropyl alcohol was then added to harden the isoniazid-loaded sodium alginate nano-size range particles. The prepared ATDs loaded nanoparticles were then collected by centrifugation at 10000rpm for 30min, washed twice with isopropyl alcohol and once with water (27)

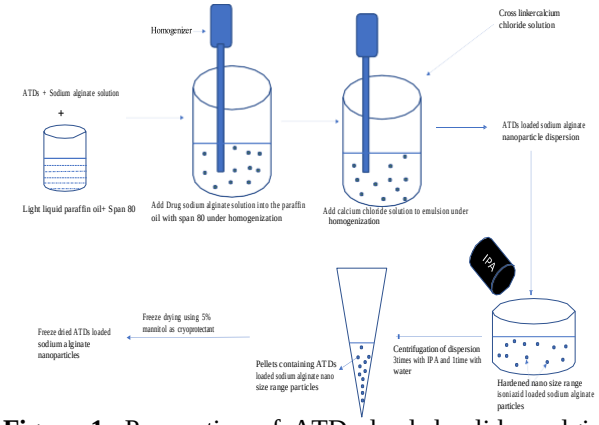

Figure 1: Preparation of ATDs loaded solidum alginate nanoparticles using the Emulsification/internal gelation technique

Table 1: Batches of composition of ATDs loaded solidum alginate nanoparticles

S. No.	Name of ingredient	Amount of ingredient			
		Isoniazid nanoparticles (SN1)	Rifampicin nanoparticles (SN2)	Pyrazinamide nanoparticles (SN3)	Moxifloxacin Hcl nanoparticles (SN4)
1	Isoniazid (mg)	75	-	-	-
2	Rifampicin mg)	-	150	-	-
3	Pyrazinamide (mg)	-	-	400	-
4	Moxifloxacin Hcl (mg)	-	-	-	400
5	Sodium alginate (%w/v)	4.22	3.85	4.99	4.39
6	Volume of sodium alginate (ml)	3	3	15	14
7	Volume of the 500mM $Cacl_2$ (ml)	1.5	1.5	7.5	6
8	Homogenization speed (rpm)	10635	12756	10000	10000
9	Homogenization time (min.)	5	5	5	10
10	Probe sonication amplitude (%)	40	40	50	40
11	Probe sonication time (min.)	1	1	1	4
12	Span 80 (ml)	0.5	0.5	2.5	2
13	Light liquid paraffin (ml)_	10	10	30	30

1.2.2 Freeze drying of the ATDs loaded sodium alginate nanoparticles

The pellets of the ATDs loaded sodium alginate nanoparticles obtained from the centrifugation step were redispersed in the distilled water and freeze-dried using the 5% w/v mannitol as cryoprotectant at pressure of 0.01 mbar throughout the process (4).

1.2.3 *In-vitro* characterization parameters

1.2.3.1 Physical appearance

The physical appearance of the prepared dispersion was investigated by visual observation of the tailored formulation

1.2.3.2 Percentage yield

The percentage yield of the dried formulation was assessed employing the below equation:

$$\text{Percentage yield} = \frac{\text{Practical amount of nanoparticles}}{\text{Amount of drug and excipients}} \times 100 \quad \text{.....(i)}$$

1.2.3.3 Percentage drug entrapment and percentage drug loading

The percentage drug entrapment of the encapsulated antituberculosis drug in the sodium alginate nanoaprticles was accessed in the centrifugation step. Accurately measured freeze-dried ATDs laoded sodium alginate nanoparticle was transferred to a beaker containing 10ml of a mixture of the solvent water: methanol in 8:2, sonicated for 1min and heat at 50°C. The solution was centrifuged at 10,000 rpm for 30 minutes. The supernatant was diluted with methanol, and the sample was scanned between 200 to 400 nm using a UV spectrophotometer (n=3) (27, 28). The percentage drug entrapment and percentage drug loading of the sample was determined using the following equation:

$$\text{Percentage drug entrapment} = \frac{\text{Initial drug} - \text{Drug in supernatent}}{\text{Initial drug}} \times 100 \quad \text{.....(ii)}$$

$$\text{Percentage drug loading} = \frac{\text{Amount of entrapped drug}}{\text{Amount of the nanoparticle taken}} \times 100 \quad \text{.....(iii)}$$

1.2.3.4 Particle size analysis

The average particle size (estimated as hydrodynamic diameter) of freeze-dried ATDs loaded sodium alginate nanoparticles was accessed using the using the dynamic light scattering approach. The investigation was performed at a fixed angle of 90° and a temperature of 25°C. The freeze-dried sample was diluted 100 times using distilled water and bath sonicated for 5 minutes. The activity was performed in triplicate manner (29).

1.2.3.5 Zeta Potential

The laser light-scattering technique was used to determine the zeta-potential of the prepared nanoparticles using a zetasizer (Zetasizer Nano ZS90; Malvern Instruments Ltd, UK). Samples were diluted in distilled water and placed in the capillary measurement cell, with the cell position adjusted. The activity was performed in triplicate manner (30).

1.2.3.6 FTIR

FTIR spectrum of the drug and freeze-dried ATDs loaded sodium alginate nanoparticles was noted using the FTR Perkin Elmer Spectrum 2. The sample was analyzed scanning ranging from 400–4000 cm^{-1} at a resolution of 4 cm−1 at room temperature (31).

1.2.3.7 DSC

DSC analysis of the drug and freeze-dried ATDs loaded sodium alginate nanoparticles was accessed to investigate the thermal behaviours of drug in bulk form as well as in the nanoparticle formulation. Thermograms of the isoniazid, rifampicin, pyrazinamide, moxifloxacin HCl and freeze-dried ATDs loaded sodium alginate nanoparticles were obtained using a DSC SETARAM (Model: SETLINE DSC). Each sample was weighed and transferred to the aluminium pan followed by crimped employing the crimper and heated from 30 °C to 400 °C at a heating rate of 10°C min^{-1}. The DSC thermogram was captured and investigated (31).

1.2.3.8 X-ray diffraction

X-ray diffraction (XRD) of the drug and freeze-dried ATDs loaded sodium alginate nanoparticles was accessed to investigate the crystalline and amorphous nature of drug and test formulation employing an PXRD Empyrean (Malvern). The XRD patterns were collected over an angular range 2θ (5°–60°) (32).

1.2.3.9 Transmission electron microscopy

The surface architecture of the freeze-dried ATDs loaded sodium alginate nanoparticles was determined using the HRTEM-JEM 2100 plus. The freeze-dried ATDs loaded nanoparticles was diluted 100 times with the distilled water, sonicated for 1min and transferred to the carbon film-covered copper grid followed by air-dried for 24 h. Images were captured to identify the shape to the nanoparticles (34).

1.2.4 Preparation of combined ATDs loaded nanoparticles containing DPI

The freeze-dried nanoparticles were manually combined with the carrier in a weight ratio using a geometrical dilution technique. The formulations listed in Table 2 were prepared by physically blending the components using geometric mixing, and following each component was processed through a sieve #60. The formulations showed that suitable flow characteristics were further accessed. The prepared formulation was labelled and stored till further use (34).

Table 2: Composition of the ATDs loaded nanoparticles containing DPI

	Formulation code		
	SNDPI1	**SNDPI2**	**SNDPI3**
Isoniazid loaded nanoparticles	Equivalent to 75mg of The isoniazid	Equivalent to 75mg of the isoniazid	Equivalent to 75mg of The Isoniazid
Rifampicin loaded nanoparticles	Equivalent to 150mg of the rifampicin	Equivalent to 150 mg of the rifampicin	Equivalent to 150mg of the Rifampicin
Pyrazinamide loaded nanoparticles	Equivalent to 400mg of the Pyrazinami De	Equivalent to 400 mg of the Pyrazinami de	Equivalent to 400mg of the Pyrazinami De
Moxifloxacin Hcl loaded nanoparticles	Equivalent to 400 mg of the moxifloxacin Hcl	Equivalent to 400 mg of the moxifloxacin Hcl	Equivalent to 400 mg of the Moxifloxacin Hcl

Nanoparticles: Lactose carrier ratio (w/w)	1:10	-	-
Nanoparticles: Leucin carrier ratio (w/w)	-	1:10	-
Nanoparticles: Mannitol carrier ratio (w/w)	-	-	1:10

1.2.5 *In-vitro* characterization of the combined ATDs loaded nanoparticles containing DPI

1.2.5.1 Physical appearance

The prepared combined ATDs loaded nanoparticles containing DPI were visually observed.

1.2.5.2 Micromeritic properties

Compressibility index (Carrs index)

Weigh precisely 0.1 g of each combined drug loaded nanoparticle containing dry powder inhaler that has been put into a 10ml graduated cylinder. Level the powder gently without compacting it, and then measure the apparent volume that hasn't settled. The activity was performed in triplicate manner (35).

$$\text{Bulk density} = \frac{\text{Weight of powder}}{\text{Bulk Volume}} \quad \ldots\ldots\ldots\ldots \text{(iv)}$$

It is the proportion of the powder's total mass to its tapped volume. Accurately measure 0.1 g of each drug loaded nanoparticle containing dry powder inhaler was transferred into a 10 ml graduated cylinder of a tap density tester. This device was operated for a predetermined number of taps until the powder bed volume reached a minimum, at which point the formula was applied: (35)

$$\text{Tapped density} = \frac{\text{Weight of powder}}{\text{Tapped Volume}} \quad \ldots\ldots\ldots\ldots \text{(v)}$$

The compressibility index (CI) measures a powder's propensity to consolidate (i.e., unite to form a solid form).

$$\text{Carrs index} = \frac{\text{Tapped density} - \text{Bulk density}}{\text{Tapped density}} \times 100 \quad \ldots\text{(vi)}$$

Hausner's Ratio is a number that is correlated to the flow ability of a powder.

Hausner's ratio= Tapped density/Bulk Density…..(vii)

Hausner's ratio (<1.25) indicates better flow properties than higher ones (>1.25).

1.2.5.3 *In-vitro* drug release study

The in-vitro release of combined ATDs loaded nanoparticles containing DPI incorporating nanoparticles and a blend of the pure drug was investigated using the dialysis membrane. The dialysis membrane (12-14KDa) was activated by soaking in the hydroalcoholic solution overnight. The blend of the antituberculosis drug and the dry powder formulation of each combined ATDs loaded nanoparticles containing DPI was dispersed in the enzyme-free simulated lung fluid pH 7.4 separately. The dispersion was added to the washed dialysis membrane, and both end of the being-filled dialysis membrane was tiled using the thread and hand in the beaker containing 10ml of simulated lung fluid without enzymes pH 7.4. The dialysis membrane containing beaker was maintained at 37°C and 100rpm over a magnetic stirrer. The sample were withdrawn at different time intervals like 0hr, 0.25hr, 0.5hr, 1hr, 2hr, 4hr, 8hr, 10hr, 12hr, 24hr and replace with the fresh drug release medium. The withdrawn sample was diluted with the methanol solvent and analyzed using UV spectroscopy. The activity was performed in triplicate manner (34).

1.2.5.4 *In-vivo* pharmacokinetic Study

The assessment of the pharmacokinetics of combined ATDs loaded nanoparticles containing DPI and blend of API DPI was accomplished using the rat animal model. According to the Institutional Animal Ethics Committee's (IAEC) Committee for Prevention, Control, and Supervision of Experimental Animals, permission number VCTE/IAEC/PH/24/016 rules, experiments were carried out. The combined ATDs loaded nanoparticles DPI and blend of API DPI were administered through pulmonary rout using an appropriate insufflator device. Rats were divided into the following groups for the pharmacokinetic study: Group 1: Blend of API; Group 2: combined ATDs loaded nanoparticles DPI. Blood was drawn via retroorbital plexuses 0.5, 2, 4, 6, 12, and 24 hours after the formulation was administered and stored in an EDTA tube followed by centrifuged for 20 minutes at 1000 rpm. The plasma was separated and filtered using a membrane filter (0.22µm). Drug estimation in plasma was carried out utilizing a developed high performance liquid chromatography (HPLC) technology. The pharmacokinetic parameters w computed, including the area-under-the-plasma drug concentration over time curve, peak plasma concentration (Cmax), and time to achieve Cmax (Tmax) Using pK solver software (36-38).

1.2.5.4.1 HPLC method of analysis

The chromatographic separation was accomplished using the Revers phase C18 (250 mm × 4.6 mm, perfectSil Target ODS-3 5 µm particle size, MZ Analytical, Germany). The mobile phase comprise of water (solvent A) and methanol (solvent B) in ratio of (A:B) 95:05 v/v. The mobile phase was run at flow rate of 1.5 mL min^{-1} for 12 min, than linear gradient to 20:80 v/v until 15 min and was kept until 23 min. At 23 min, the mobile phase was changed to the initial composition and was maintained until 26 minutes before the next injection. The injection volume was 100µ(39). The monitoring wavelengths were 254 nm for INH, PZA, and Moxifloxacin, and 336 nm for RIF. The sample preparation

includes the addition of the methanol solvent in the biological samples. The samples were centrifuge at 5000rpm for 10min. The supernatant was suitably diluted with diluent, filtered using the 0.22µ membrane filter paper, and injected in the HPLC.

1.2.5.5 Statistical analysis

Statistical analysis was accomplished employing the Graph Pad Instat Software (GraphPad Software, La Jolla, CA). The pharmacokinetic data were accessed employing the Student's unpaired t-test. Difference with considered statistically significant

1.3 Result and discussion

1.3.1 Development of the ARDs loaded nanoparticles

The current study involves the preparation of the encapsulation of Isoniazid, Rifampicin, Pyrazinamide, and Moxifloxacin Hcl in the sodium alginate nanoparticle, employing the emulsification/internal gelation method. Following this, the aqueous polymeric solution was emulsified into an oil phase with surfactant, and calcium chloride was added as a cross-linker. Calcium chloride crystals provide the calcium for the gelation step. The release of calcium from the calcium complex results in gelation and the production of Ca-polysaccharide. Calcium ions immobilize labile biological components by cross-linking the polysaccharide residues.

1.3.2 *In-vitro* characterization of ATDs (Isoniazid, Rifampicin, Pyrazinamide, and Moxifloxacin Hcl) Loaded Sodium Alginate nanoparticle

Table 3: In vitro characterization parameters of ATDs (Isoniazid, Rifampicin, Pyrazinamide and Moxifloxacin Hcl) loaded sodium alginate nanoparticle

S. No.	Name of ingredient	Formulation			
		Isoniazid nanoparticles (SN1)	Rifampicin nanoparticles (SN2)	Pyrazinamide nanoparticles (SN3)	Moxifloxacin Hcl nanoparticles (SN4)
1	Physical appearance	Uniform, Homogenous dispersion	Uniform, Homogenous dispersion	Uniform, Homogenous dispersion	Uniform, Homogenous dispersion
2	Percentage yield (%)	94.498 ±0.312	93.789 ±0.871	94.498 ±0.312	96.660 ±0.249
3	Percentage drug entrapment (%)	76.632 ±0.448	75.260±0.101	76.797 ±0.293	77.252±0.086
4	Percentage drug loading (%)	21.261 ±0.254	32.036 ±0.352	14.196 ±0.458	16.480 ±0.017
5	Particle size (nm)	199.167 ±0.777	221.77 ±1.645	273.157 ±4.117	250.327 ±0.818
6	Zeta Potential (mv)	-30.447 ±0.689	-29.210 ±0.608	-29.153 ±1.778	-31.193 ±0.900
7	PDI	0.161 ±0.003	0.187 ±0.005	0.179 ±0.007	0.180 ±0.001

ATDs (Isoniazid (INH), Rifampicin (RIF), Pyrazinamide (PYRA), and Moxifloxacin (MOXI) Hcl) were encapsulated separately into sodium alginate nanoparticles because of bioadhesives and well-established pulmonary safety profile of sodium alginate. The ATDs loaded sodium alginate nanoparticles were prepared using the calcium ion to facilitate the sustained release of the encapsulated drug. The prepared ATDs (INH-, RIF-, PYRA, and MOXI) loaded sodium alginate nanoparticles were uniform and free from the Aggregation. Following freeze drying, the percentage recovery of the INH-, RIF-, PYRA, and MOXI-loaded nanoparticles were 94.498±0.312%, 93.789±0.871%, 94.498±0.312%, and 96.660±0.249%, respectively. The percentage drug entrapment and drug loading of these formulations were 76.632±0.448%, 7 5 .260±0.101%, 7 6 .797±0.293%, 77.252±0.086%; 2 1 .261±0.254%, 32.036±0.352%, 14.196±0.458%, 16.480±0.017% respectively, Similarly the particle size and PDI of these formulations were 199.167±0.777nm, 221.77±1.645nm, 273.157±4.117 and 250.327±0.818; 0.164±0.003, 0.192±0.005, 0.185±0.007, 0.179±0.001. The zeta potential of these formulations was -31.20±0.689 mv, -29.60±0.608 mv, -31.0±1.778 mv, and -32.0±0.900mv.

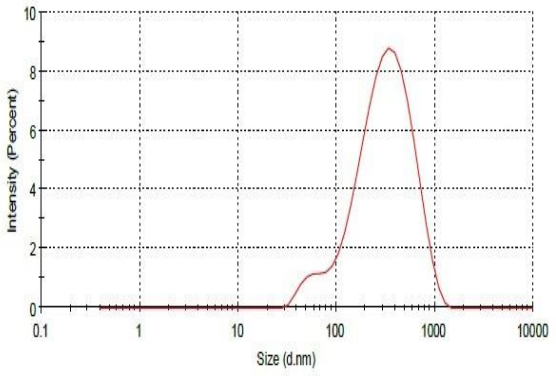

Figure 2: Particle size distribution of moxifloxacin Hcl laoded nanoparticles

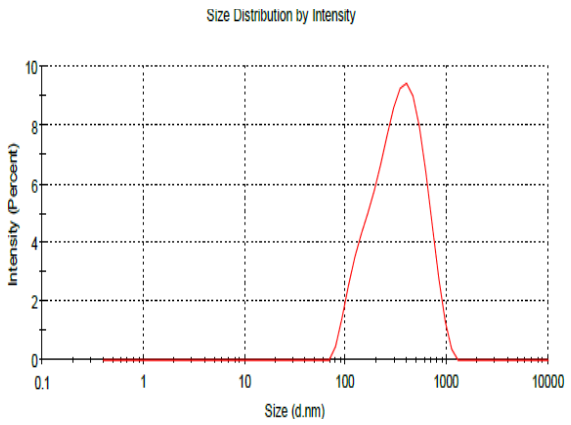

Figure 3: Particle size distribution of pyrazinamide loaded nanoparticles

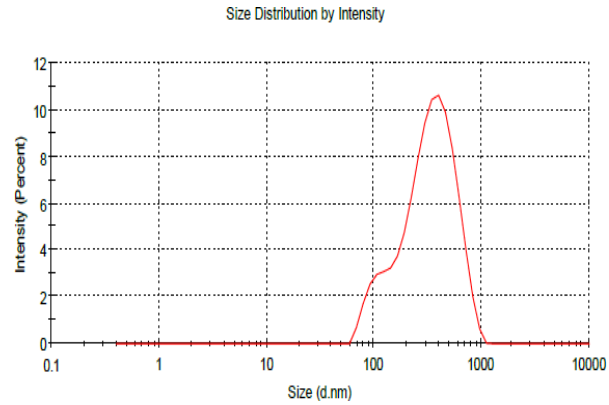

Figure 4: Particle size distribution of rifampicin loaded nanoparticles

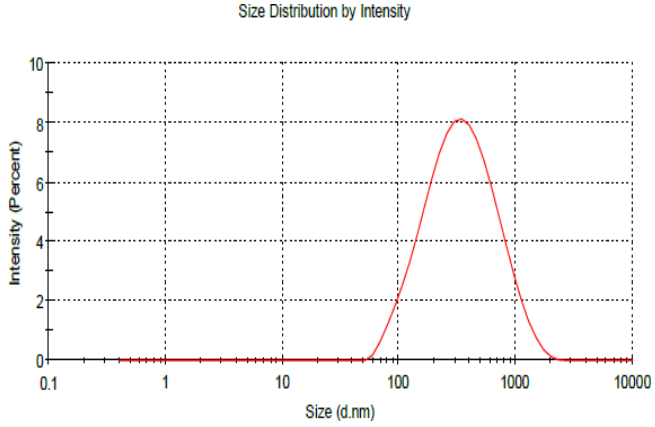

Figure 5: Particle size distribution of isoniazid loaded nanoparticles

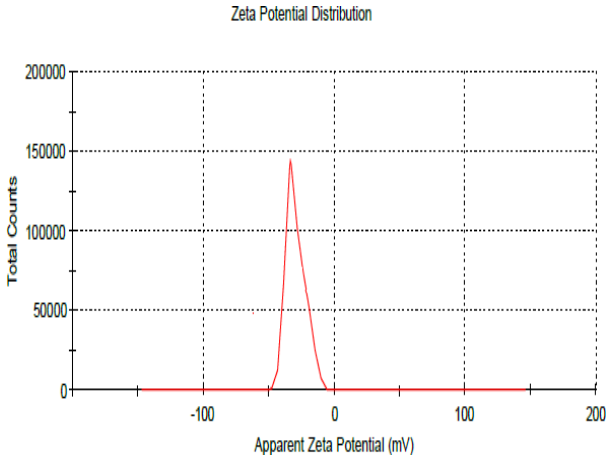

Figure 6: Zeta potential distribution of rifampicin laoded nanoparticles

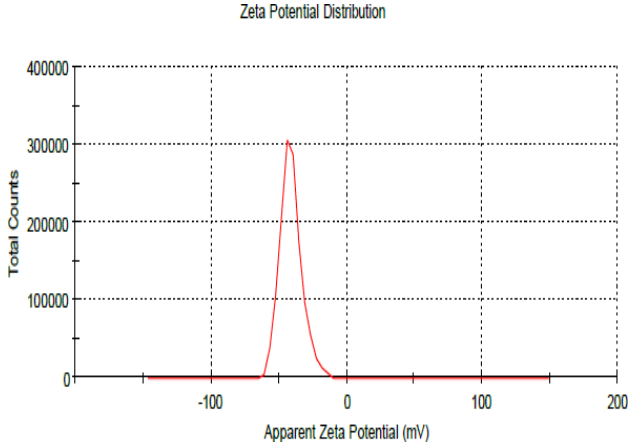

Figure 7: Zeta potential distribution of isoniazid laoded nanoparticles

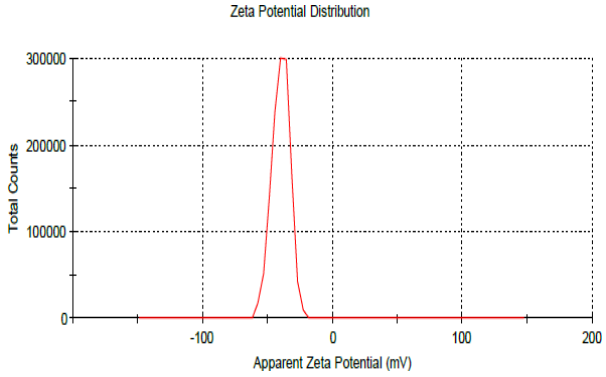

Figure 8: Zeta potential distribution of moxifloxacin laoded nanoparticles

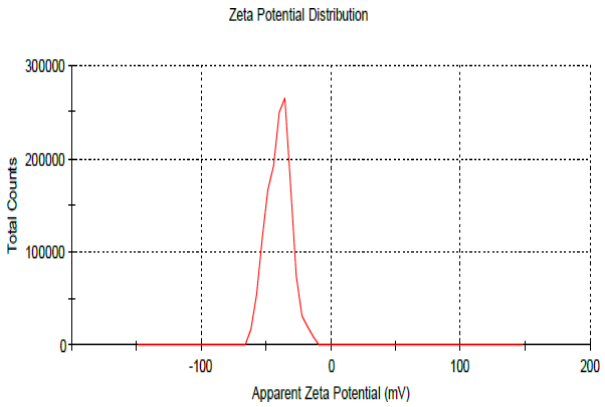

Figure 9: Zeta potential distribution of pyrazinamide loaded nanoparticles

1.3.3 FTIR spectroscopy

FTIR spectrum of the drug isoniazid, rifampicin, Pyrazinamide, moxifloxacin Hcl, isoniazid loaded nanoparticles, rifampicin loaded nanoparticles, pyrazinamide loaded nanoparticles, and moxifloxacin Hcl loaded nanoparticles are shown in Figure 11-17. FTIR spectrum of the isoniazid demonstrated the characteristics peaks at wavenumber of 3103.40cm^{-1} (Bonded NH and C-H), 1661.97cm^{-1} (Amide I (CLO stretching), 1552.35cm^{-1} (N–H bending of secondary amide group), and 13632.91cm^{-1} (NH_2 Deformation) (40,41). FTIR spectrum of the rifampicin demonstrated the characteristics peaks at wavenumber of 1693.54cm^{-1} (C=O (Acetyl stretching), 3284.41cm^{-1} (C-H stretching), 1693.54cm^{-1} (C=N (asymmetric stretching), 1615.62cm^{-1} (N-H (Amide bending), 1427.31cm^{-1} (C=C (stretching), and 1236.7cm^{-1} (C-N (stretch) (42). FTIR spectrum of the pyrazinamide demonstrated the characteristics peaks at wavenumber of 3409.98cm^{-1} (N–H assym: stretching), 3146.57cm^{-1} (C–H stretching), 1703.03cm^{-1} (C=O stretching), 1607.43cm-1 (C-C (ring) stretching), 1434.10cm-1 (C-N (ring) assym stretching), 1375.51cm^{-1} (C-N (ring) sym stretching) (43,44). FTIR spectrum of the moxifloxacin demonstrated the characteristics peaks at wavenumber of 2689.89cm^{-1} (Stretching $(N\text{-}H_2)^+$, 1706.11cm^{-1} (Stretching (C=O); COOH), 1624.13-1517cm-1 (Stretching (C=O); phenyl breathing), 1455.58-1351.34cm^{-1} -CH; deformations of CH_2) (45). FTIR spectrum of all four individual drug loaded nanoparticle indicated the shifting of the characteristic peaks of the drug like isoniazid, rifampicin, moxifloxacin and pyrazinamide indicated the compatibility between the drug and excipients as well as the encapsulation of the drug in the nanoparticles (46).

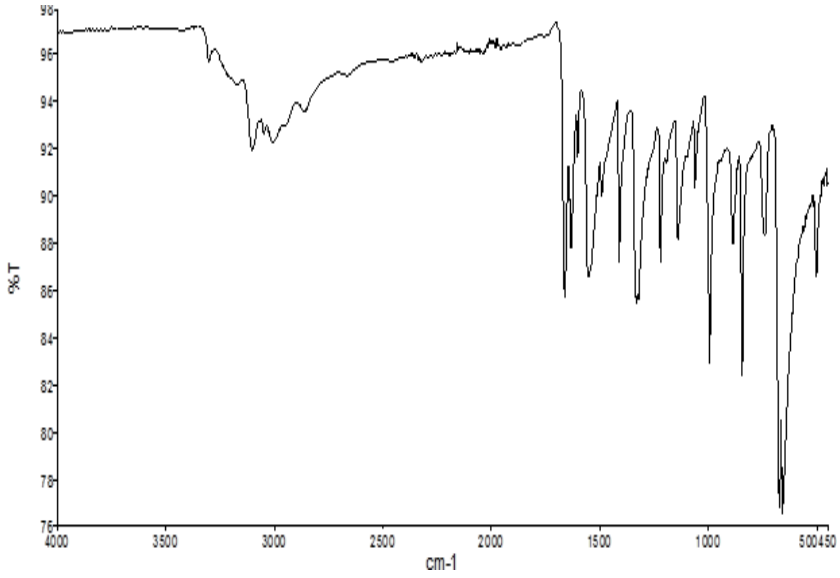

Figure 10: FTIR spectrum of the drug isoniazid

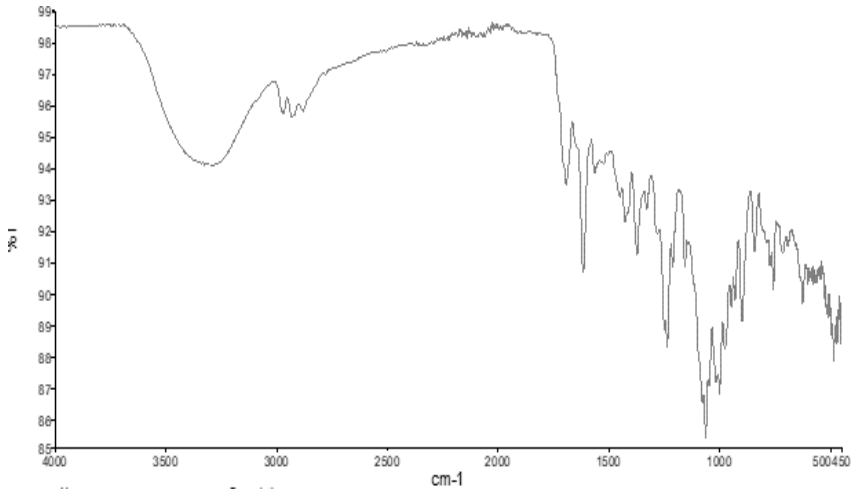

Figure 11: FTIR spectrum of the drug rifampicin

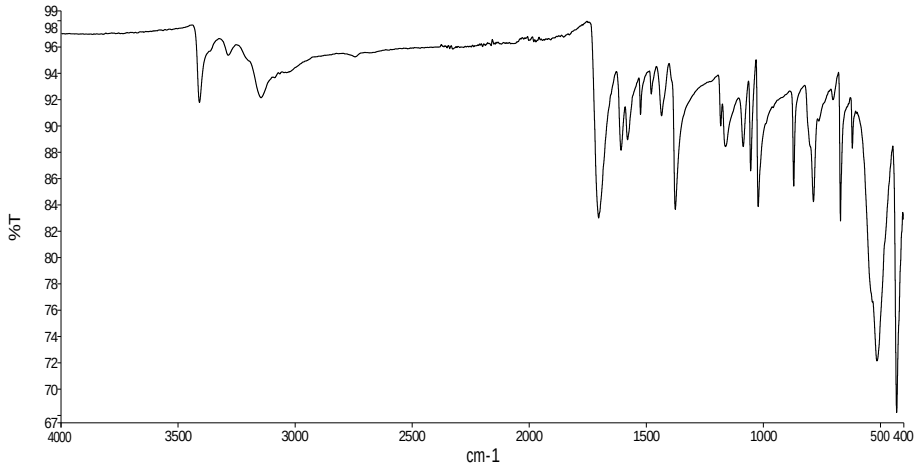

Figure 12: FTIR spectrum of the drug pyrazinamide

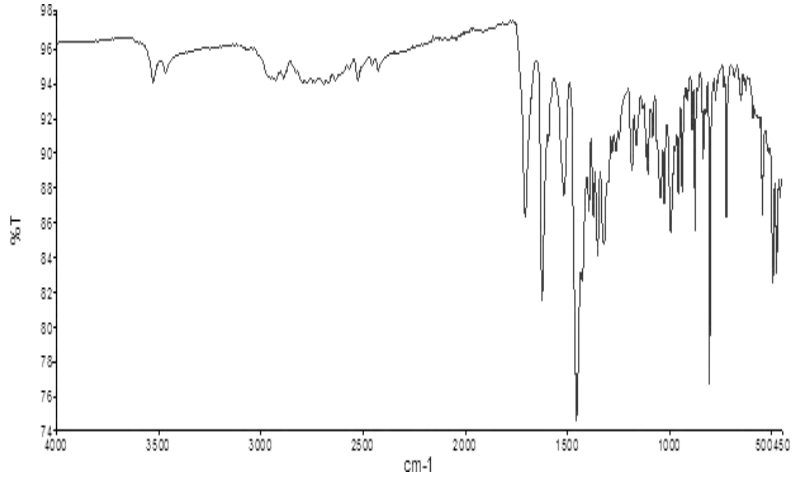

Figure 13: FTIR spectrum of the drug moxifloxacin Hcl

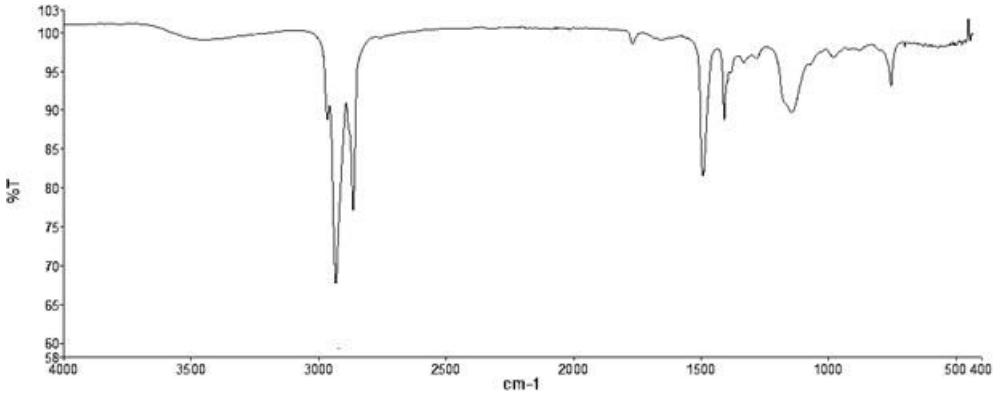

Figure 14: FTIR spectrum of pyrazinamide loaded sodium alginate nanoparticles

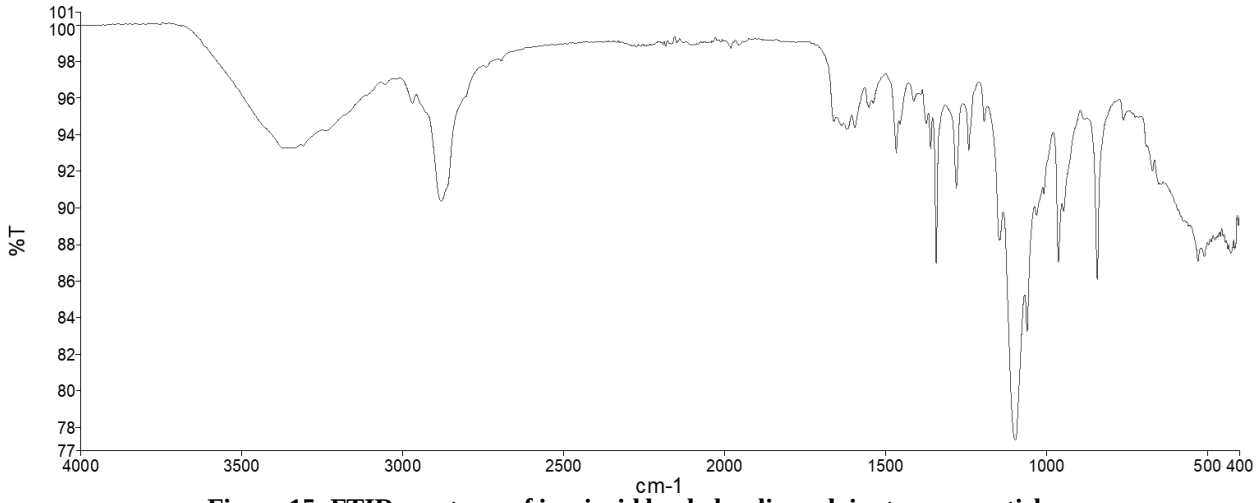

Figure 15: FTIR spectrum of isoniazid loaded sodium alginate nanoparticle

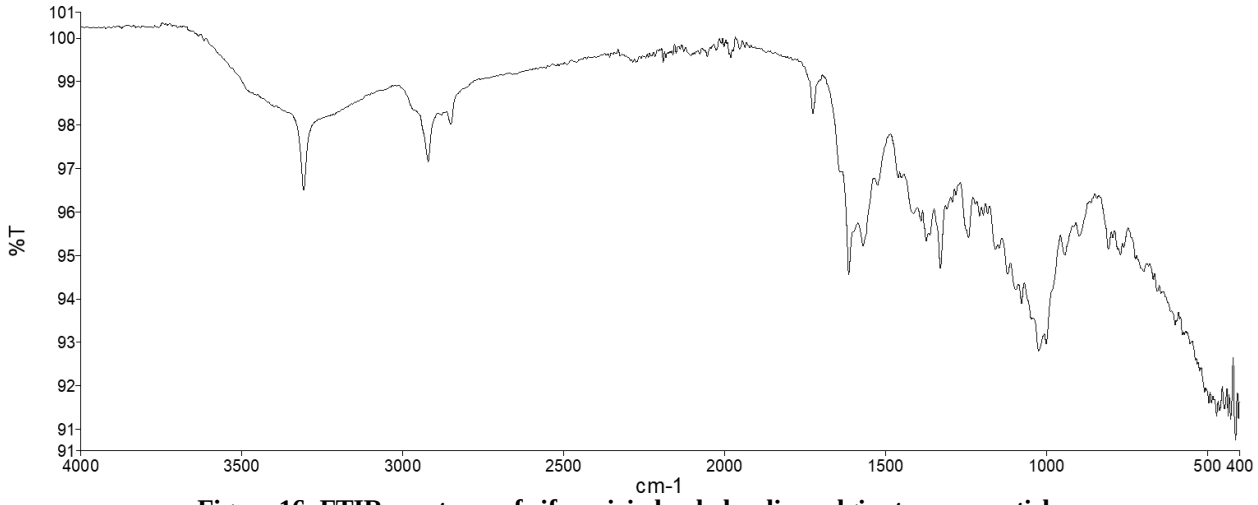

Figure 16: FTIR spectrum of rifampicin loaded sodium alginate nanoparticle

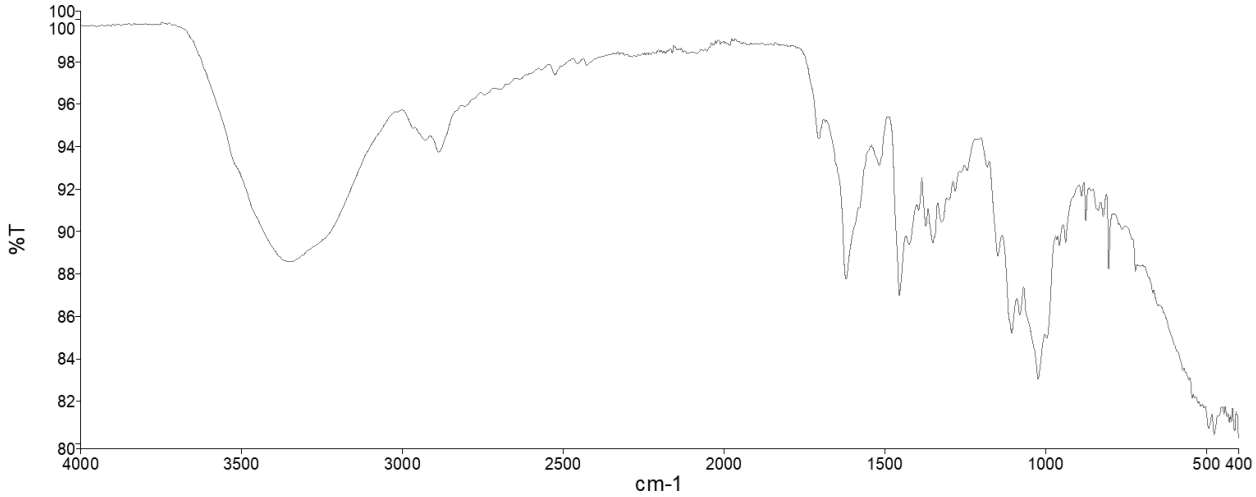

Figure 17: FTIR spectrum of moxifloxacin Hcl loaded sodium alginate nanoparticles

1.3.4 DSC analysis

DSC thermogram of the drug isoniazid, rifampicin, Pyrazinamide, moxifloxacin Hcl, isoniazid loaded nanoparticles, rifampicin loaded nanoparticles, pyrazinamide loaded nanoparticles, and moxifloxacin Hcl loaded nanoparticles are shown in Figure 18-25. The DSC endotherm of isoniazid, moxifloxacin Hcl and Pyrazinamide showed a sharp melting endotherm at 172.223◦C (47), 232.85°C (48), and 190.186 °C (49). DSC thermogram of rifampicin demonstrated thermal decomposition process of Rifampicin at 258.99 °C. The thermal events observed on the DSC curve are consistent with the reported literature (50). DSC thermogram of reach drug loaded nanoparticles indicated intensity of the peak of each drug was diminished in the formulation, indicating a molecular-level dispersion of drug and complete solubilization within the matrix, indicating the encapsulation of drug in the nanoparticles (31).

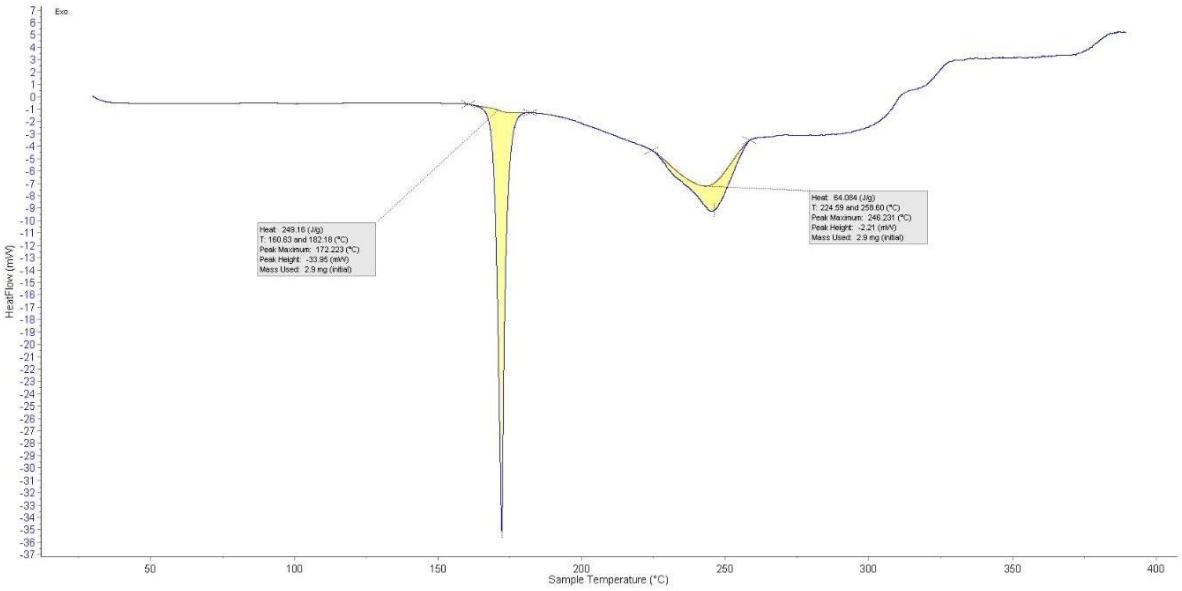

Figure 18: DSC thermogram of isoniazid

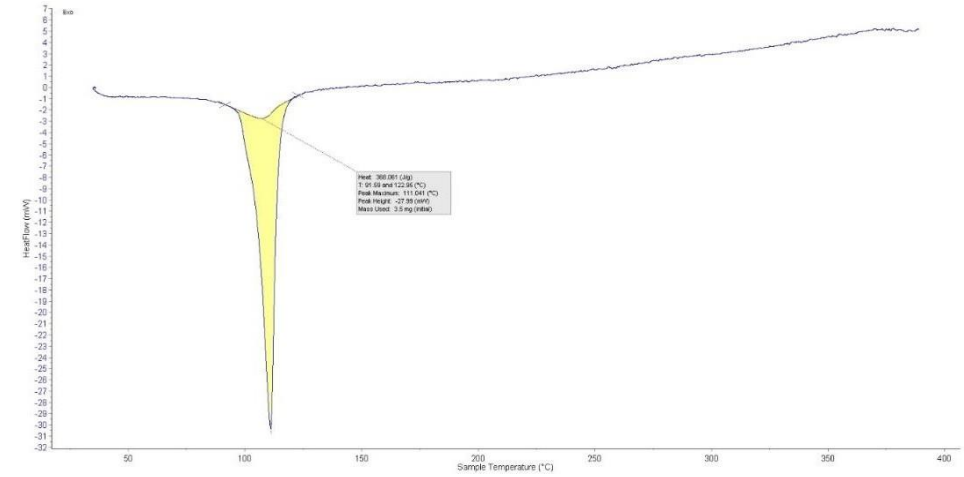

Figure 19: DSC thermogram of isoniazid loaded sodium alginate nanoparticles

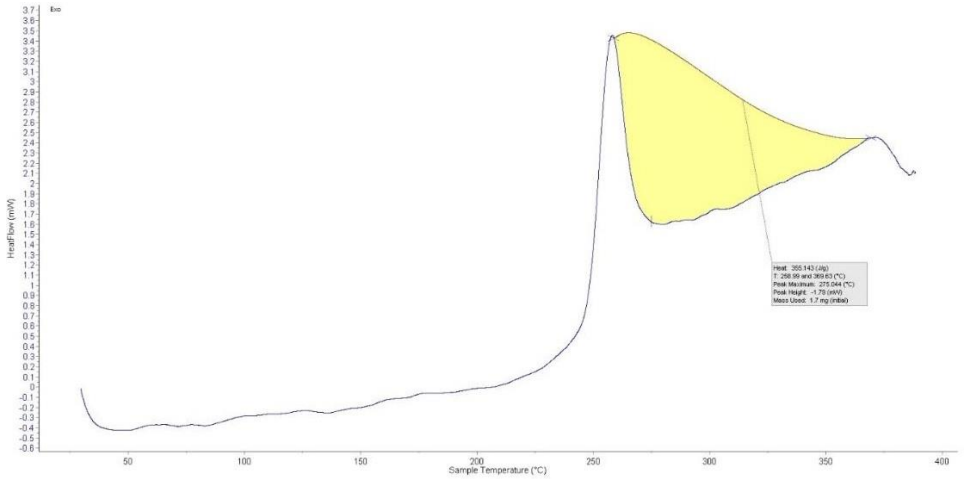

Figure 20: DSC thermogram of rifampicin

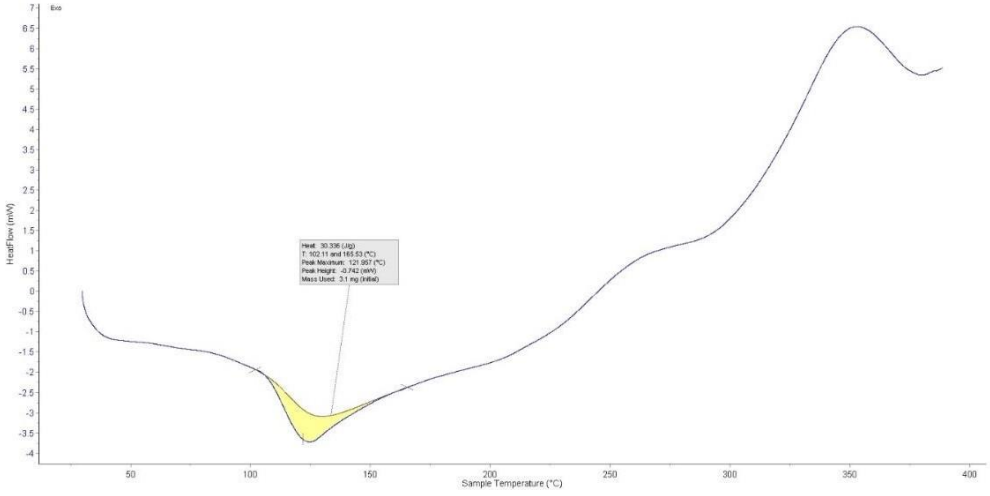

Figure 21: DSC thermogram of rifampicin loaded sodium alginate nanoparticles

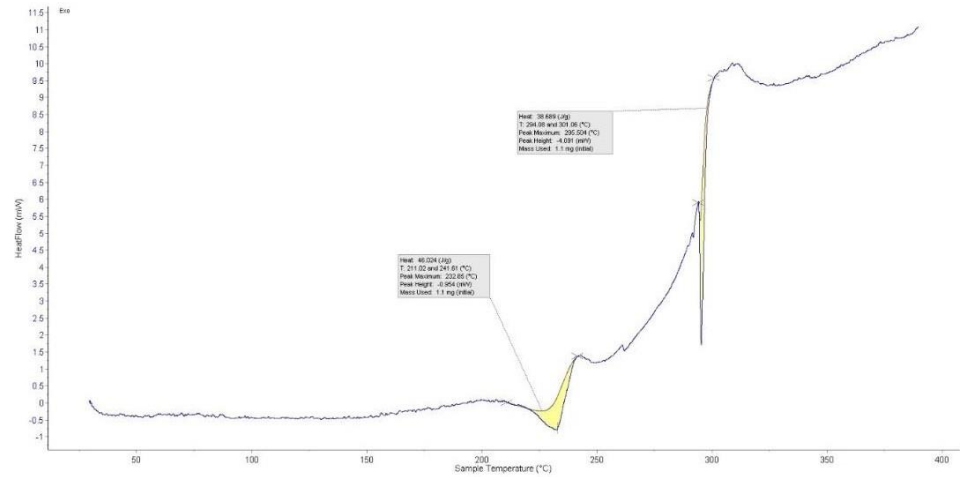

Figure 22: DSC thermogram of Moxifloxacin Hcl

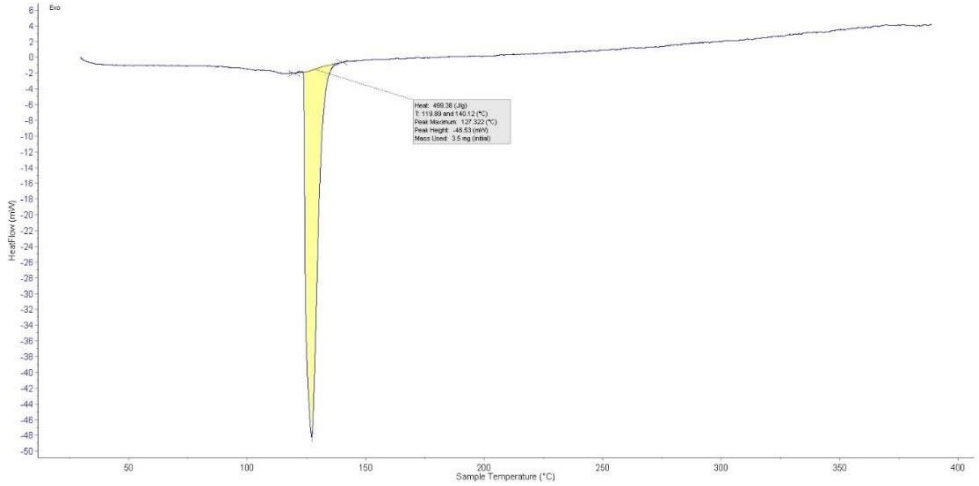

Figure 23: DSC thermogram of Moxifloxacin Hcl loaded sodium alginate nanoparticles

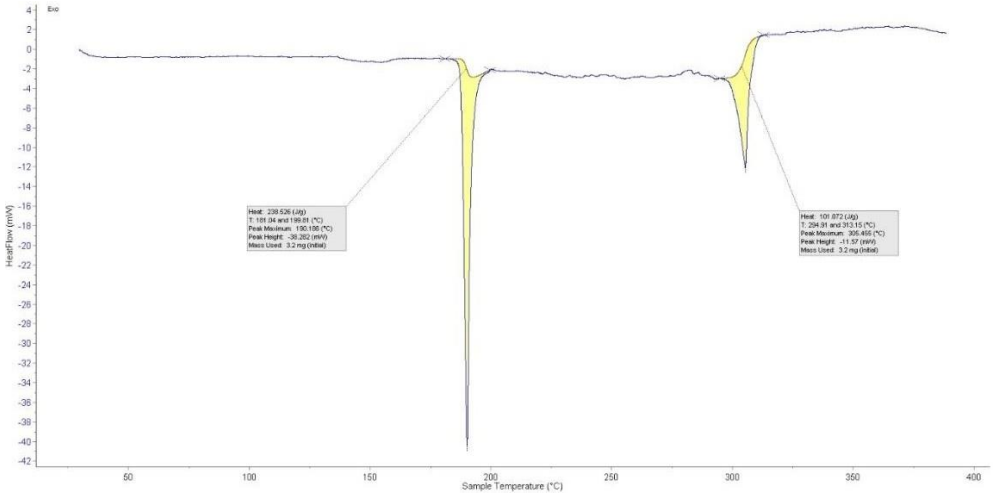

Figure 24: DSC thermogram of Pyrazinamide

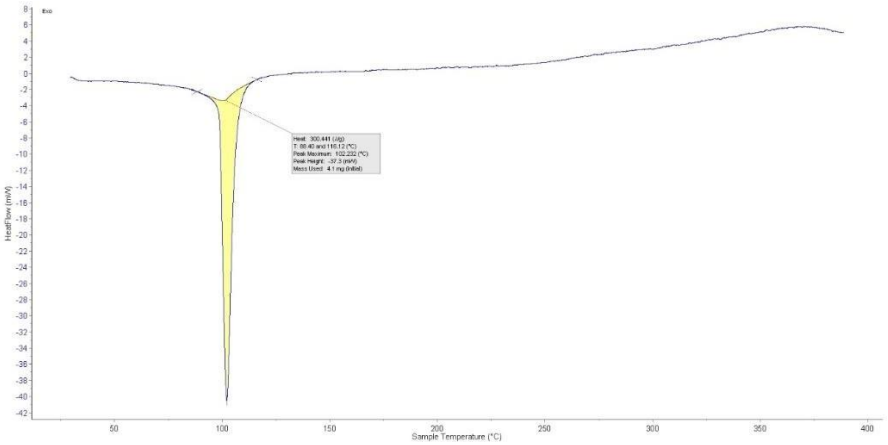

Figure 25: DSC thermogram of Pyrazinamide loaded sodium alginate nanoparticles

1.3.5 X-ray diffraction spectroscopy

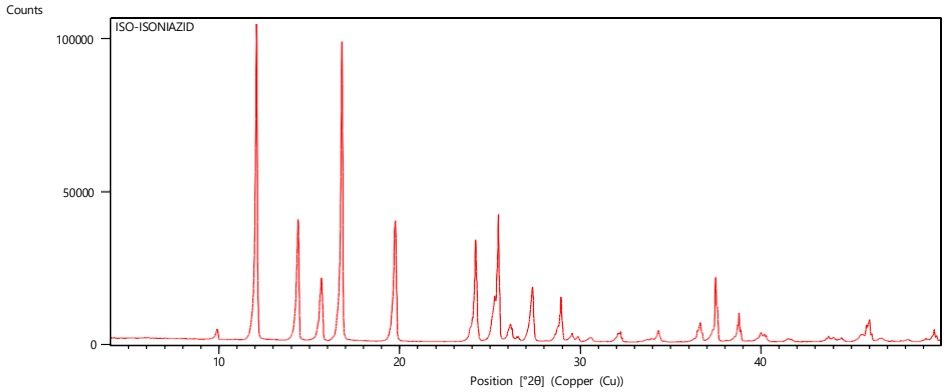

Figure 26: XRD of isoniazid

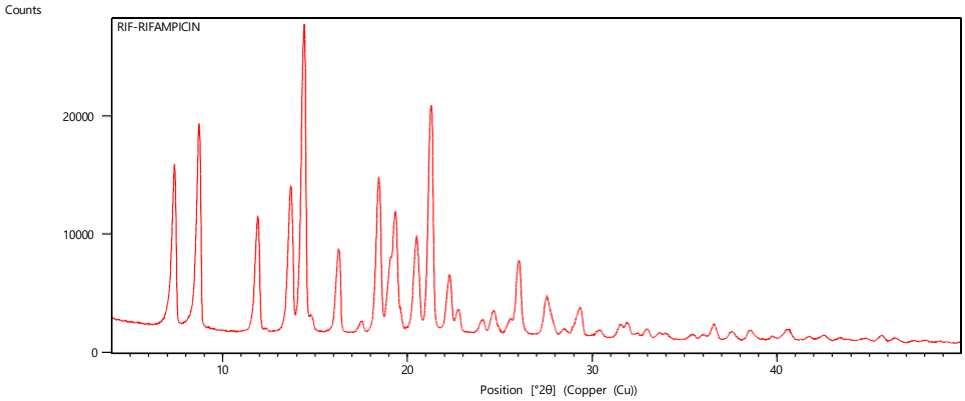

Figure 27: XRD of rifampicin

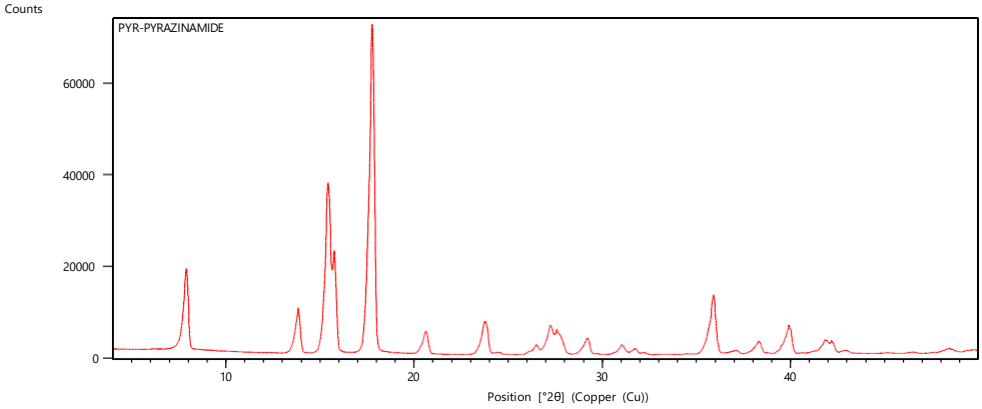

Figure 28: XRD diffractogram of pyrazinamide

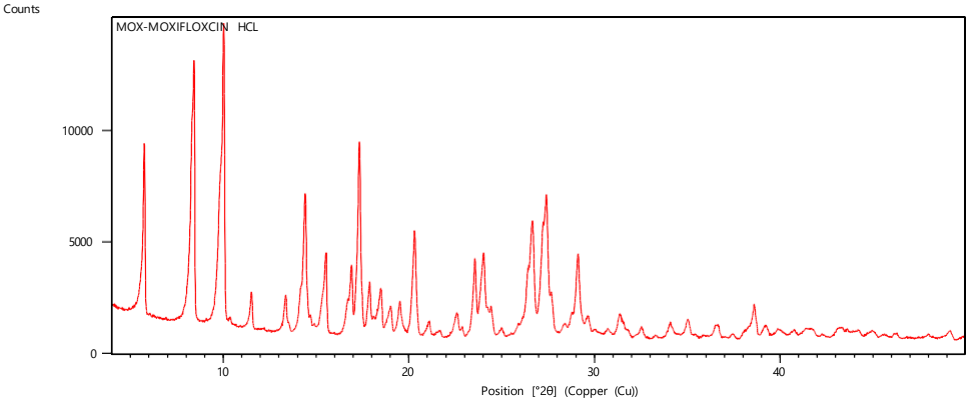

Figure 29: XRD diffractogram of moxifloxacin Hcl

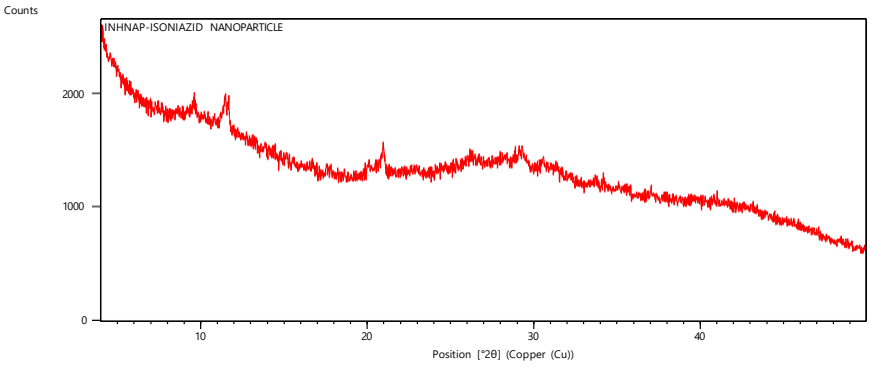

Figure 30: XRD diffractogram of isoniazid loaded nanoparticles

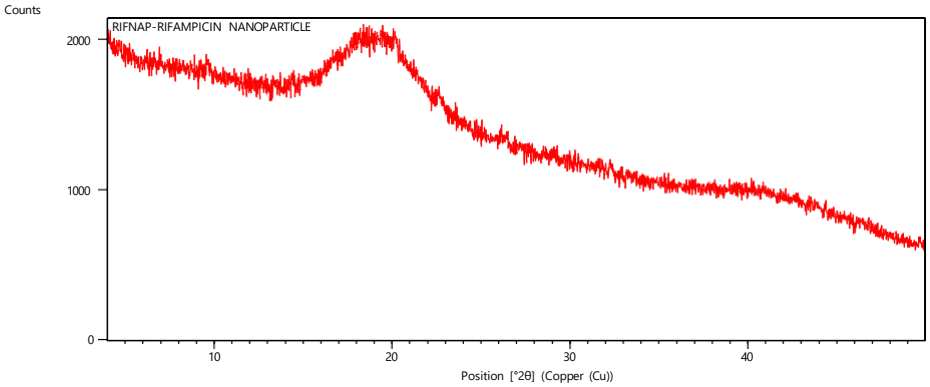

Figure 31: XRD diffractogram of rifampicin loaded nanoparticles

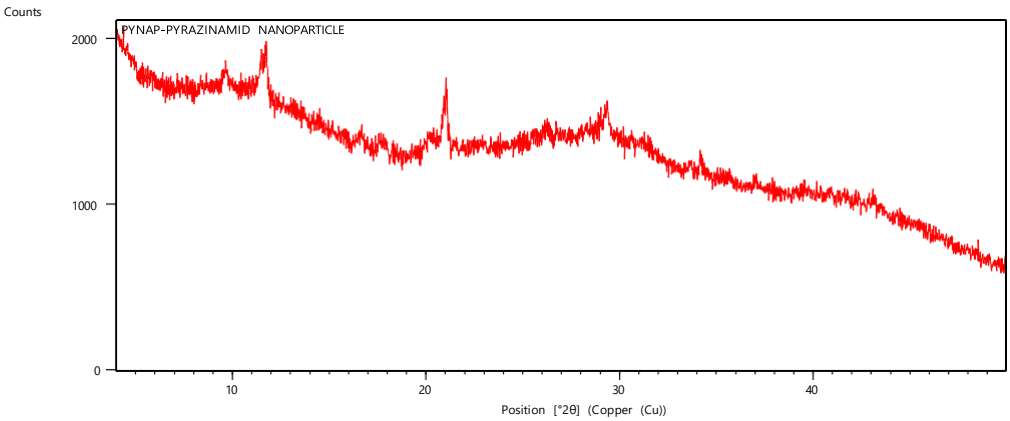

Figure 32: XRD diffractogram of pyrazinamide loaded nanoparticles

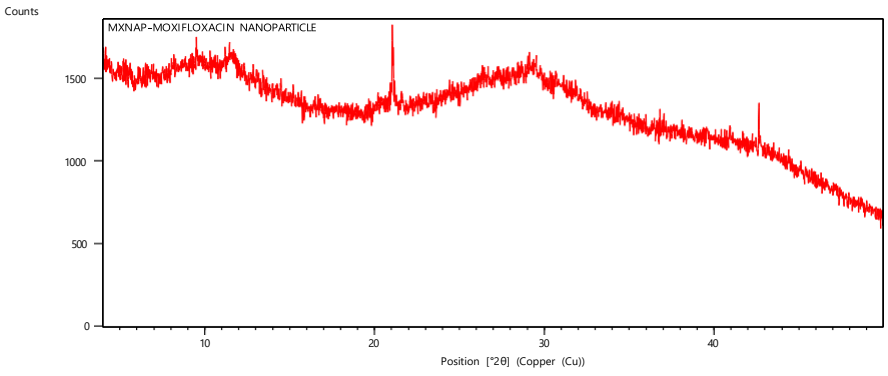

Figure 33: XRD diffractogram of moxifloxacin Hcl loaded nanoparticles

XRD patterns of isoniazid, rifampicin, pyrazinamide, and moxifloxacin Hcl, isoniazid loaded sodium alginate nanoparticles, rifampicin loaded sodium alginate nanoparticles, pyrazinamide loaded sodium alginate nanoparticles, and moxifloxacin Hcl loaded sodium alginate nanoparticles were given in Figure 26-33. The XRD pattern of Rifampicin

revealed its crystalline character from the major peaks at 2θ =14.3586 (46). Isoniazid (Fig. 2, curve 2a) demonstrated peaks ranging 12to 50° indicated its crystalline nature (40). The diffraction pattern of pure Pyrazinamide demonstrated sharp peaks at 17.72° 2θ, which demonstrated the crystalline behaviour of pyrazinamide (51). The X-ray diffractogram of moxifloxacin showed a distinct peak at 10.015 at 2θ, indicating its crystalline nature (52). The XRD diffractogram of the ALG nanoparticles attributed the absence of the sharp peaks, indicating the dispersion or encapsulation of the drug in nanoparticles matrix (46).

1.3.6 Transmission electron microscopy

The HR-TEM images of the isoniazid loaded nanoparticles, rifampicin loaded nanoparticles, pyrazinamide loaded nanoparticles, and moxifloxacin Hcl loaded nanoparticles were shown In Figure 34-37.

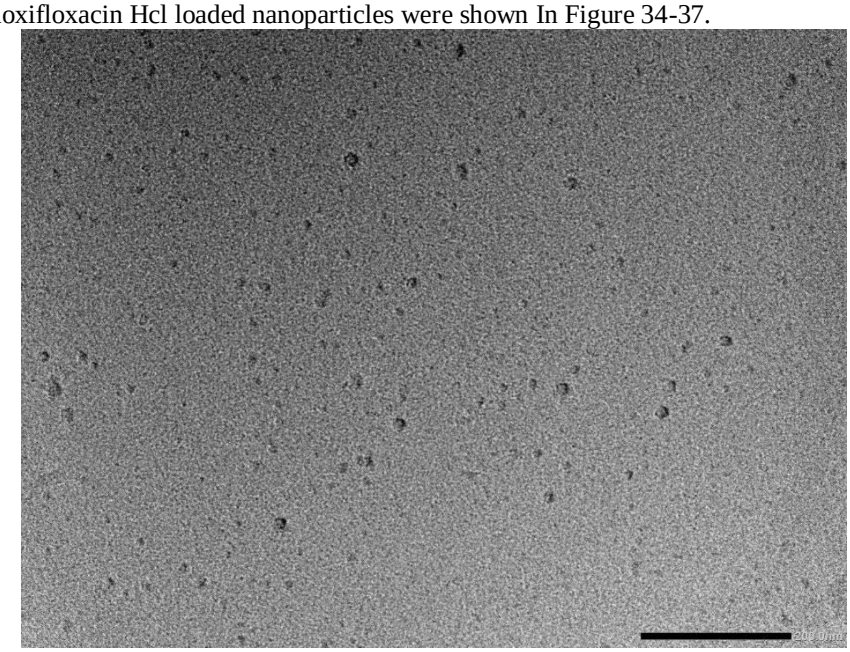

Figure 34: HR-TEM image of rifampicin loaded nanoparticles

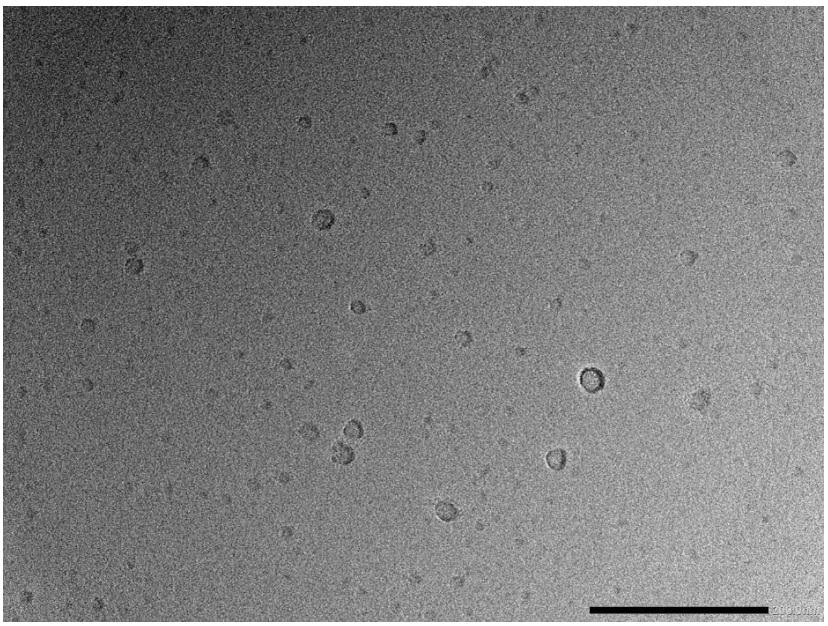

Figure 35: HR-TEM image of isoniazid loaded nanoparticles

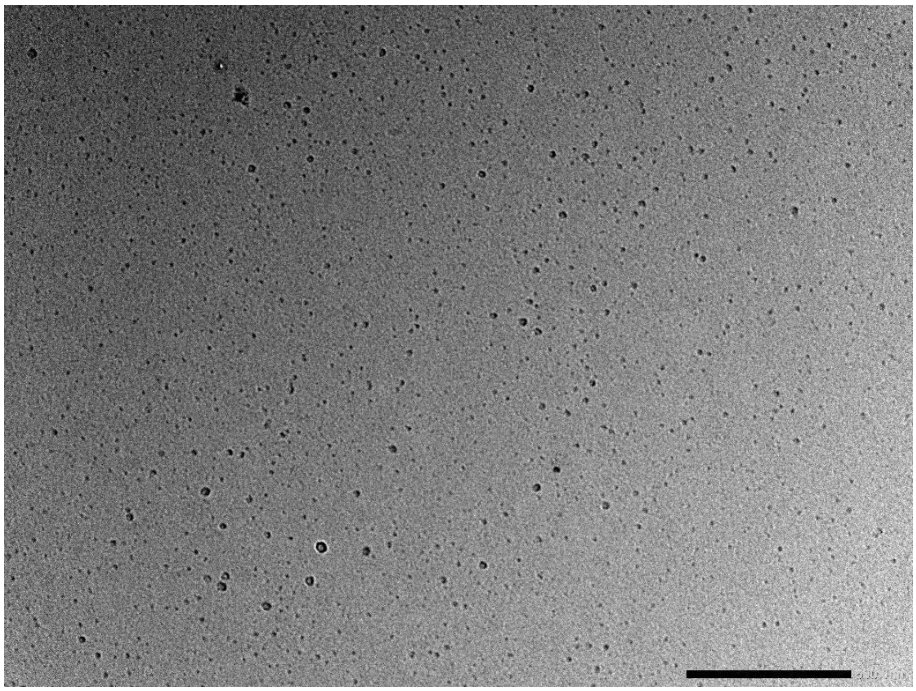

Figure 36: HR-TEM image of moxifloxacin loaded nanoparticles

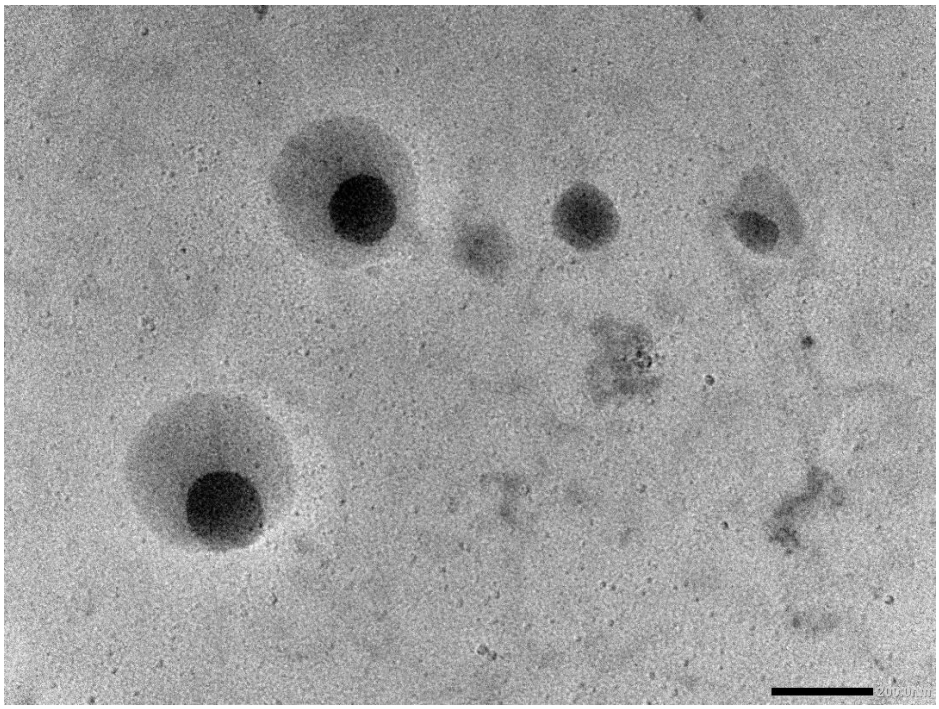

Figure 37: HR-TEM image of Pyrazinamide loaded nanoparticles

Figure 34-37 shows that all formulations, including isoniazid-loaded nanoparticles, rifampicin-loaded nanoparticles, pyrazinamide-loaded nanoparticles, and moxifloxacin HCl-loaded nanoparticles, have a spherical shape with homogeneous distribution, in agreement with the results obtained in the particle size analyzer.

1.3.7 Development of combined ATDs (Isoniazid, Rifampicin, Pyrazinamide, and Moxifloxacin Hcl) Loaded sodium alginate nanoparticle DPI

The next activity involves the incorporation of freeze-dried nanoparticles into DPI carrier. In the current investigation, all four ATDs (Isoniazid, Rifampicin, Pyrazinamide and Moxifloxacin Hcl) loaded freeze-dried nanoparticles were mixed with each carrier (lactose, leucin and mannitol) in a 1:10w/w ratio. The carrier in the DPI formulation is responsible for maintaining the formulation's good flow characteristics (53). This may also lead to improved aerosolization behavior of the formulation because of increased flowability brought on by a higher drug dispersion (54).

1.3.8 *In-vitro* characterization of combined ATDs (Isoniazid, Rifampicin, Pyrazinamide and Moxifloxacin Hcl) loaded sodium alginate nanoparticle combined DPI

Table 4: *In-vitro* characterization of combined ATDs (Isoniazid, Rifampicin, Pyrazinamide and Moxifloxacin Hcl) loaded sodium alginate nanoparticle combined DPI

S.No.	Test parameter	Formulation		
		SNDP1	SNDPI2	SNDPI3
1	Physical appearance	Uniform, Homogenous, free flowing Powder	Uniform, Homogenous, free flowing Powder	Uniform, but aggregation of particles
2	Carrs index	2.521±0.250	15.303±1.747	34.037±5.121
3	Hausner ratio	1.026±0.026	1.181±0.024	1.522±0.118
4	Angel of repose	24.560±0.236	31.560±0.178	38.480±0.084

The prepared batches of the ATDs loaded nanoparticles containing DPI formulation were uniform, free, and homogenous, except the DPI formulation comprises of the mannitol as a carrier. The DPI formulation containing mannitol demonstrated the aggregation of the particles. Therefore, it is crucial to keep an eye on the formulation's flow and reaggregation characteristics during the formulation of DPI preparation. Investigation of the flow property and deaggregation behaviour is an important parameter during the preparation of DPI. The flow property of the DPI formulation was investigated through the micrometric properties. The value of the all flow characteristic parameters for the DPI formulation comprising the lactose as a carrier demonstrated better than the DPI formulation comprising the leucin and mannitol as a carrier.

The in vitro drug release of INH, PZA, RIF, and MHCl from the combined ATDs loaded nanoparticles containing DPI (SNDPI1) was examined in contrast to the pure API blend in combination. The blend of API demonstrated the release of approximately 95.460±0.921% of the isoniazid within 60 minutes due to the high-water solubility of the isoniazid. were dissolved in 60 minutes due to the increased water solubility of pure INH. However, the combined ATDs loaded nanoparticles containing DPI (SNDPI1) showed a bimodal release, with a burst release within 3–4 hours and a nearly sustained release behaviour over the 24 hours (Figure 38). Similarly, the drug release profile of the remaining three drug rifampicin, pyrazinamide and moxifloxacin Hcl from the blend of API demonstrated the immediate release profile 87.897±0.267% 91.605±0.816%, and 85.989±0.569%. All three drugs, rifampicin, pyrazinamide and moxifloxacin Hcl, release from the sodium alginate nanoparticles DPI in a sustained manner.

1.3.8.1 *In-vitro* drug release study

Table 5: Percentage drug release of the combined ATDs loaded nanoparticles containing DPI (SNDPI1) and blend of API

Time(hr.)	Percentage drug release of isoniazid	Percentage drug release of rifampicin	Percentage drug release of pyrazinamide	Percentage drug release of moxifloxacin Hcl	Percentage drug release of isoniazid from SNDPI1	Percentage drug release of rifampicin from SNDPI1	Percentage drug release of pyrazinamide from SNDPI1	Percentage drug release of moxifloxacin Hcl form SNDPI1
0	0.000±0.00	0.000±0.000	0.000±0.00	0.000±0.000	0.000±0.000	0.00±.00	0.000±0.00	0.000±0.000
0.25	8.775±0.092	17.668±0.042	8.248±0.025	6.490±0.015	5.052±0.031	3.678±0.70	5.416±0.074	2.500±0.060
0.5	34.696±0.132	50.284±0.426	28.129±0.077	13.035±0.031	12.700±0.217	6.294±0.049	10.730±0.091	6.423±0.071
1	95.460±0.921	79.240±0.183	45.003±0.255	60.426±0.751	18.587±0.083	9.086±0.018	25.299±0.089	12.442±0.052
2		87.897±0.267	91.605±0.816	71.774±0.225	28.434±0.098	14.6260.058	34.386±0.977	14.193±0.049
4				85.989±0.569	41.033±0.193	19.165±0.048	47.217±0.643	21.710±0.64
8					49.161±0.900	32.087±0.286	57.689±0.569	33.391±0.605

10					60.896±1.316	59.110±0.450	64.734±0.198	60.840±0.509
12					76.502±0.796	76.115±0.605	72.164±0.470	79.881±0.644
24					80.766±0.520	78.454±0.478	74.420±0.297	84.591±0.808

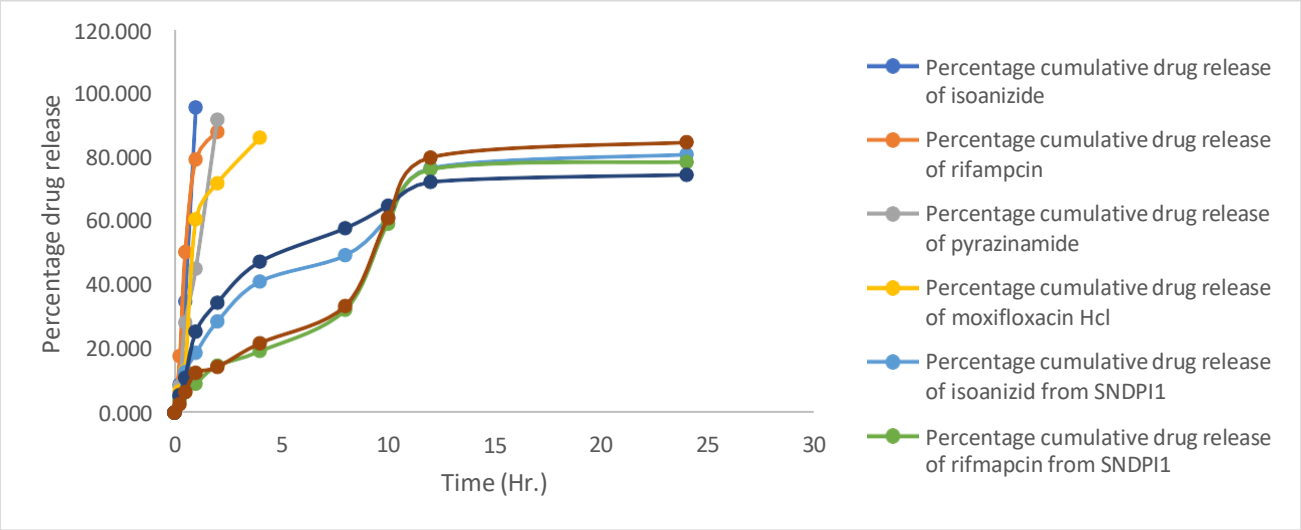

Figure 38: Comparison of percentage drug release from the combined ATDs loaded nanoparticles containing DPI (SNDPI1) formulation and blend of API

1.3.8.2 *In-vivo* Pharmacokinetics

The in vivo outcomes of both the blend of ATDs DPI and the combined ATDs loaded nanoparticles containing DPI (SNDPI1) formulation are assessed after pulmonary administration in order to confirm whether co-administration of ATDs (Isoniazid, Rifampicin, Pyrazinamide, and Moxifloxacin Hcl) loaded sodium alginate nanoparticles in DPI (Formulation: SNDPI1) could augment ATDs' therapeutic efficacy. Figure 39 shows the average concentration-time profiles in the lung after inhaling combined ATDs loaded nanoparticles containing DPI (SNDPI1) and the blend of ATDs drug DPI.
Furthermore, DPI containing sodium alginate nanoparticles may sustain drug levels in the lungs for up to 24 hours after combined ATDs loaded nanoparticles containing DPI (inhalation. However, post administration of the blend of ATDs DPI, there was a noticeable drop in the drug level in the lung. This decrease in the lung's pure drug level was attributed to the quick removal of pure ATDs from the pleural cavity into the bloodstream (55).

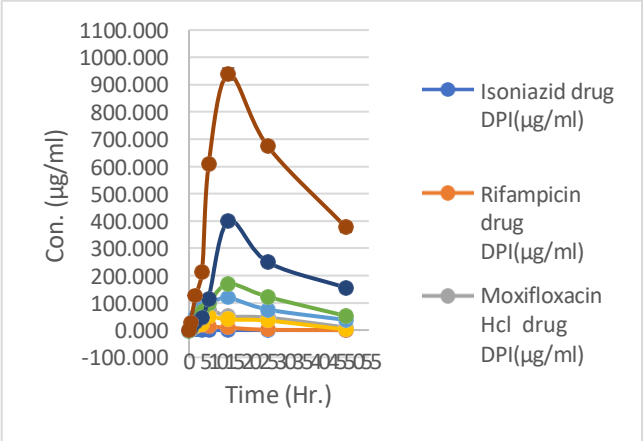

Figure 39: Mean concentration-time profile after inhalation of plain ATDs and the combined ATDs loaded nanoparticles containing DPI (SNDPI1) in lung

The pharmacokinetic parameters of a blend of ATDs and the combined ATDs loaded nanoparticles containing DPI (SNDPI1) are summarized in Table 6. Entrapping ATDs within sodium alginate nanoparticles combined in DPI formulation augmented drug accumulation within lung tissue in a significant manner. The mean residence time (MRT) of all four drugs in SNDPI1 was between 34-46 hours. The AUC value in the lung for formulation SNDPI1 was higher than the AUC of a blend of ATDs. The higher AUC value for the optimized SNDPI1 formulation may be due to higher accumulation and less alveolar clearance of drug-loaded nanoparticles than the plain drug.

Table 6: Pharmacokinetic parameters of blend of ATDs DPI and ATDs loaded nanoparticle combined in DPI

	Blend of ATDs DPI				ATDs loaded nanoparticles combined in DPI			
Parameter	**Isoniazid**	**Rifampicin**	**Pyrazinamide**	**Moxifloxacin Hcl**	**Isoniazid**	**Rifampicin**	**Pyrazinamide**	**Moxifloxacin Hcl**
t1/2 (h)	2.323±0.090	5.088±0.405	14.660±0.605	8.706±0.142	21.729±0.281	20.804±1.613	27.392±2.671	27.492±1.416
Tmax (h)	2±0	4±0	6±0	6±0	12±0	12±0	12±0	12±0
Cmax (µg/ml)	0.787±0.073	18.322±1.639	73.591±2.894	48.895±2.826	117.757±3.011	169.305±9.967	400.563±11.327	938.617±21.779
AUC 0-t (µg/ml *h)	2.645±0.417	200.849±2.795	1776.181±71.423	1258.140±73.824	3510.515±238.389	4931.916±188.782	10548.825±148.745	28218.672±209.865
MRT (h)	3.999±0.205	9.097±0.432	23.549±0.700	17.951±0.100	34.588±0.457	34.719±2.415	46.810±3.973	44.865±2.189

1.4 Conclusion

In the current study, the four antituberculosis drugs isoniazid, rifampicin, pyrazinamide, and moxifloxacin Hcl was encapsulated in sodium alginate nanoparticle. All four ATDs loaded sodium alginate nanoparticles in combination were mixed with the carrier and transformed in the DPI formulation. The in vivo pharmacokinetic study demonstrated that the combined ATDs loaded sodium alginate nanoparticle containing DPI formulation demonstrated better pharmacokinetic parameters than the blend of API DPI.

REFERENCE

1. Global tuberculosis report 2022. Geneva: World Health Organization; 2022. Licence: BY-NC-SA 3.0 IGO. ⟨https://www.who.int/teams/global- tuberculosis-programme/tb-reports/global-tuberculosis-report-2022⟩. [Accessed on 26 May 2023].

2. Mandal S, Rao R, Joshi R. Re-estimating tuberculosis incidence and mortality in India during 2011-2022: a modelling study. Indian J. Community Med, 2023;48: 436–42.

3. Rai PY, Sansare VA, Warrier DU, Shinde UA. Formulation, characterization and evaluation of inhalable effervescent dry powder of Rifampicin nanoparticles. Indian J. Tuberc, 2023;70(1):49–58.

4. Mukhtar M, Csaba N, Robla, S, Varela-Calviño R, Nagy A, Burian K, Kókai D, Ambrus R. Dry Powder Comprised of Isoniazid-Loaded Nanoparticles of Hyaluronic Acid in Conjugation with Mannose-Anchored Chitosan for Macrophage-Targeted Pulmonary Administration in Tuberculosis. Pharm, 2022;14(8):1543.

5. Paul PK, Nakpheng T, Paliwal H, Prem Ananth K, Srichana T. Inhalable solid lipid nanoparticles of levofloxacin for potential tuberculosis treatment. Int J Pharm, 2024:660;124309.

6. Abdelghany S, Parumasivam T, Pang A, Roediger B, Tang P, Jahn K, Chan H-K. Alginate modified-PLGA nanoparticles entrapping amikacin and moxifloxacin as a novel host-directed therapy for multidrug-resistant tuberculosis J Drug Deliv Sci Technol, 2019;52:642-651

7. Chan JG, Chan HK, Prestidg CA, Denman JA, Young PM, Traini D. A novel dry powder inhalable formulation incorporating three first-line anti-tubercular antibiotics. Eur J Pharm Biopharm, 2013;83(2):285–292.

8. Traini D, Young PM. Delivery of antibiotics to the respiratory tract: an update. Expert Opin Drug Deliv, 2009; 6(9):897–905.

9. Liao Q, Yip L, Cho MYT, Chow S, Chan H.K, Kwo PC, & Lam JKW. Porous and highly dispersible voriconazole dry powders produced by spray freeze drying for pulmonary delivery with efficient lung deposition. Int J pharm, 2019;560:144–154.

10. Islam MS, Saha S, Gemci T, Yan I.A, Sauret E Gu YT. Polydisperse Microparticle Transport and Deposition to the Terminal Bronchioles in a Heterogeneous Vasculature Tree. Sci Rep, 2018;8(1):16387.

11. Lee W., Loo, CY, Traini D, Young PM. Nano- and micro-based inhaled drug delivery systems for targeting alveolar macrophages. Expert Opin Drug

*Author for Correspondence: govindn@lnct.ac.in

Deliv, 2015;12(6):1009–1026.
12. Xiong MH, Bao Y, Yang XZ, Zh Y.H, Wang J. Delivery of antibiotics with polymeric particles. Adv Drug Deliv Rev, 2014;78:63–76.
13. Nemati E, Mokhtarzade, A, Panahi-Azar V, Mohammadi A, Hamishehkar H, Mesgari-Abbasi M, de la Guardi M. Ethambutol-Loaded Solid Lipid Nanoparticles as Dry Powder Inhalable Formulation for Tuberculosis Therapy. AAPS PharmSciTech, 2019;20(3).
14. Dabbagh A, Abu Kasim NH, Yeong CH, Wong TW, Abdul Rahman N. Critical Parameters for Particle-Based Pulmonary Delivery of Chemotherapeutics. J Aerosol Med Pulm Drug Deliv, 2018;31(3):139–154.
15. Finlay WH. The Mechanics of Inhaled Pharmaceutical Aerosols: An Introduction 2nd edn. (Elsevier, 2019).
16. Darquenne C. Deposition Mechanisms. J Aerosol Med Pulm Drug Deliv, 2020;33(4):181–185.
17. d'Angelo , Conte C, Miro A., Quaglia F, Ungaro F. Pulmonary drug delivery: a role for polymeric nanoparticles?. Curr Top Med Chem, 2015;15(4):386–400.
18. Wan KY, Weng J, Wong SN, Kwok PCL, Chow SF, Chow AHL. Converting nanosuspension into inhalable and redispersible nanoparticles by combined in-situ thermal gelation and spray drying. Eur J pharm biopharma 2020;149:238–247.
19. Mangal S, Gao W, Li T, Zhou QT. Pulmonary delivery of nanoparticle chemotherapy for the treatment of lung cancers: challenges and opportunities. Acta Pharmacol Sin, 2017;38(6):782–797.
20. Dandekar P, Venkataraman C& Mehra, A Pulmonary targeting of nanoparticle drug matrices. J Aerosol Med Pulm Drug Deliv, 2010;23(6):343–353.
21. Donahue N, Aca H, Wilhelm S. Concepts of nanoparticle cellular uptake, intracellular trafficking, and kinetics in nanomedicine. Adv Drug Deliv Rev, 2019;143:68–96.
22. Leong WX, Ge R. Lipid Nanoparticles as Delivery Vehicles for Inhaled Therapeutics. Biomedicines, 2022;10(9):2179.
23. Nemmar A, Hoet PH, Vanquickenborne B, Dinsdale D, Thomeer M, Hoylaerts MF, Vanbilloen H, Mortelmans L, Nemery B. Passage of inhaled particles into the blood circulation in humans. Circulation, 2002;105(4): 411–414.
24. Acosta MF, Abrahamson MD, Encinas-Basurto D, Fineman JR, Black SM, Mansour H.M. Inhalable Nanoparticles/Microparticles of an AMPK and Nrf2 Activator for Targeted Pulmonary Drug Delivery as Dry Powder Inhalers. The AAPS journal, 2020;23(1): 2.
25. Jahagirdar P, Gupta, PK, Kulkarni SP Devarajan PV. Intramacrophage Delivery of Dual Drug Loaded Nanoparticles for Effective Clearance of Mycobacterium tuberculosis. J pharm sci, 2020;109(7): 2262–2270.
26. Pandey R, Khuller GK. Chemotherapeutic potential of alginate-chitosan microspheres as anti-tubercular drug carriers. J Antimicrob Chemother, 2004;53(4):635–640.
27. Zhai P, Chen XB, Schreye DJ. An in vitro study of peptide-loaded alginate nanospheres for antagonizing the inhibitory effect of Nogo-A protein on axonal growth. Biomedical materials (Bristol, England), 2015;10(4):045016.
28. Yasmin , Chen X, Eames BF. Effect of Process Parameters on the Initial Burst Release of Protein-Loaded Alginate Nanospheres. Journal of functional biomaterials J Funct Biomate, 2019;10(3):42.
29. Dolatabadi JEN, Hamishehkar H, Valizadeh H. Development of dry powder inhaler formulation loaded with alendronate solid lipid nanoparticles: solid-state characterization and aerosol dispersion performance. Drug Dev Ind Pharm, 2015;41(9):1431–1437.
30. Manuja A, Kumar S, Dilbaghi N, Bhanjana G, Chopra M, Kaur H, Kumar R, Manuja BK, Singh SK, Yadav SC. Quinapyramine sulfate-loaded sodium alginate nanoparticles show enhanced trypanocidal activity. Nanomed, 2014;9(11): 1625–1634.
31. El-Houssiny AS, War AA, Mostafa D, Abd-El-Messieh SL, Abdel-Nour KN, Darwish MM, Khalil WA. Drug–polymer interaction between glucosamine sulfate and alginate nanoparticles: FTIR, DSC and dielectric spectroscopy studies. Adv Nat Sci Nanosci 2016;7:025014.
32. Wathoni N, Rusdi A, Febriani E, Purnama D, Daulay W, Azhary SY, Panatarani C, Joni IM, Lesmana R, Motoyama K, Muchtaridi M. Formulation and Characterization of α-Mangostin in Chitosan Nanoparticles Coated by Sodium Alginate, Sodium Silicate, and Polyethylene Glycol. J Pharm Bioallied Sci, 2019;11(4):S619–S627
33. Zimet P, Mombrú ÁW, Faccio R, Brugnini G, Miraballes I, Rufo C, Pardo H. Optimization and characterization of nisin-loaded alginate-chitosan nanoparticles with antimicrobial activity in lean beef. LWT, 2018;91.
34. Debnath SK, Saisivam S, Omri A. PLGA 50:50-Ethionamide Nanoparticles for Pulmonary Delivery: development and in vivo evaluation of dry powder inhaler, J Pharm Biomed Anal, 2017;145:854-859.
35. Thapa C, Chaudhary R. Formulation and in-vitro evaluation of sustained release matrix tablets of Domperidone. JUCMS, 2020;08 (2):15-22.
36. Garg T, Goyal AK, Rath G Murth RS. Spray-dried particles as pulmonary delivery system of anti-tubercular drugs: design, optimization, in vitro and in vivo evaluation.

Pharm Dev Technol, 2016;21(8):951–960.
37. Bhatt NB, Barau , Amin A, Baudin E, Meggi B, Silva C, Furlan V, Grinsztejn B, Barrail-Tran A, Bonnet M, Taburet AM. Pharmacokinetics of rifampin and isoniazid in tuberculosis-HIV-coinfected patients receiving nevirapine- or efavirenz-based antiretroviral treatment. Antimicrob Agents Chemother, 2014;58(6):3182–3190.
38. Tian G, Longest PW, Li X, Hindle M. Targeting aerosol deposition to and within the lung airways using excipient enhanced growth. J Aerosol Med Pulm Drug Deliv, 2013;26(5):248–265.
39. Dasht Bozorg B, Goodarzi A, Fahimi F, Tabarsi P, Shahsavari N, Kobarfard F, Dastan F. Simultaneous Determination of Isoniazid, Pyrazinamide and Rifampin in Human Plasma by High-performance Liquid Chromatography and UV Detection. Iran J Pharm Res, 2019;18(4):1735–1741.
40. Banik N, HussainA., Ramteke A, Sharma H. Maji TK. Preparation and evaluation of the effect of particle size on the properties of chitosan-montmorillonite nanoparticles loaded with isoniazid, RSC Advances, 20121;2:10519–10528
41. Brewer GA. Isoniazid. Analytical Profiles of Drug Substances, 1977;183–258.
42. Gallo GG, Radaelli P. Rifampin. Analytical Profiles of Drug Substances, 1976;467–513.
43. Eedara B, Tucker, IG, Da SC. Phospholipid-based pyrazinamide spray-dried inhalable powders for treating tuberculosis. Int J pharm, 2016;506(1-2):174–183
44. Saifullah B, Arulselvan P, Fakurazi S, Webster TJ, Bull N, Hussein M El Zowalaty M E. Development of a novel anti-tuberculosis nanodelivery formulation using magnesium layered hydroxide as the nanocarrier and pyrazinamide as a model drug. Sci Rep, 2022;12(1):14086
45. Al Omari MMH, Jaafari DS, Al-Sou'od KA, Badwan AA. Moxifloxacin Hydrochloride. Profiles of Drug Substances, Excipients and Related Methodology, 2014;299–431.
46. Thomas D, KurienThomas K, Latha MS. Preparation and evaluation of alginate nanoparticles prepared by green method for drug delivery applications. Int J Biol Macromol, 2020;154: 888–895. .
47. Rastogi R, Sultana Y, Aqil M, Ali A, Kuma S, Chuttani K, Mishra AK. Alginate microspheres of isoniazid for oral sustained drug delivery. Int J Pharm, 2007;334(1-2):71-7.
48. Gade S, Patel KK, Gupta C, Anjum MM, Deepika D, Agrawal AK, Singh S. An Ex Vivo Evaluation of Moxifloxacin Nanostructured Lipid Carrier Enriched In Situ Gel for Transcorneal Permeation on Goat Cornea. J pharm sci, 2019;108(9):2905–2916.
49. Singh A, Das SS, Ruokolainen J, Kesari K, Singh SK. Biopolymer-Capped Pyrazinamide-Loaded Colloidosomes: In Vitro Characterization and Bioavailability Studies. ACS omega, 2023;8(28): 25515–25524.
50. Bibire T, Timofte D, Danil R, Panainte AD., Yilmaz CN, Bibire N, Agoroaei L, Ghiciuc, CM. Rifampicin-Loaded PLGA/Alginate-Grafted pNVCL-Based Nanoparticles for Wound Healing. Applied Sciences, 2024;14(21):9799.
51. Verma JN, Kumar TS, Prasanthi B Ratna, JV. Formulation and Characterization of Pyrazinamide Polymeric Nanoparticles for Pulmonary Tuberculosis: Efficiency for Alveolar Macrophage Targeting. Indian j pharm sci, 2025;77(3):258–266.
52. Mudgi M, Pawar PK. Preparation and In Vitro/Ex Vivo Evaluation of Moxifloxacin-Loaded PLGA Nanosuspensions for Ophthalmic Application. Sci Pharm, 2013;81(2):591–606.
53. Zeng XM, Martin GP, Marriott C. Particulate Interactions in Dry Powder Formulation for Inhalation. CRC Press. 2000
54. Islam N, Stewart P, Larson I, Hartley P. Lactose surface modification by decantation: are drug-fine lactose ratios the key to better dispersion of salmeterol xinafoate from lactose-interactive mixtures? Pharm Res, 2004;21(3):492–499.
55. Vishwa B, Moin A, Gowda DV, Rizvi SMD, Hegazy WAH, Abu Lila AS, Khafagy ES, Allam AN. Pulmonary Targeting of Inhalable Moxifloxacin Microspheres for Effective Management of Tuberculosis. Pharm, 2021;13(1):79.